Cloud microphysics

Claudia Emde

Meteorological Institute, LMU, Munich, Germany

WS 2011/2012

Energy balance of the Earth

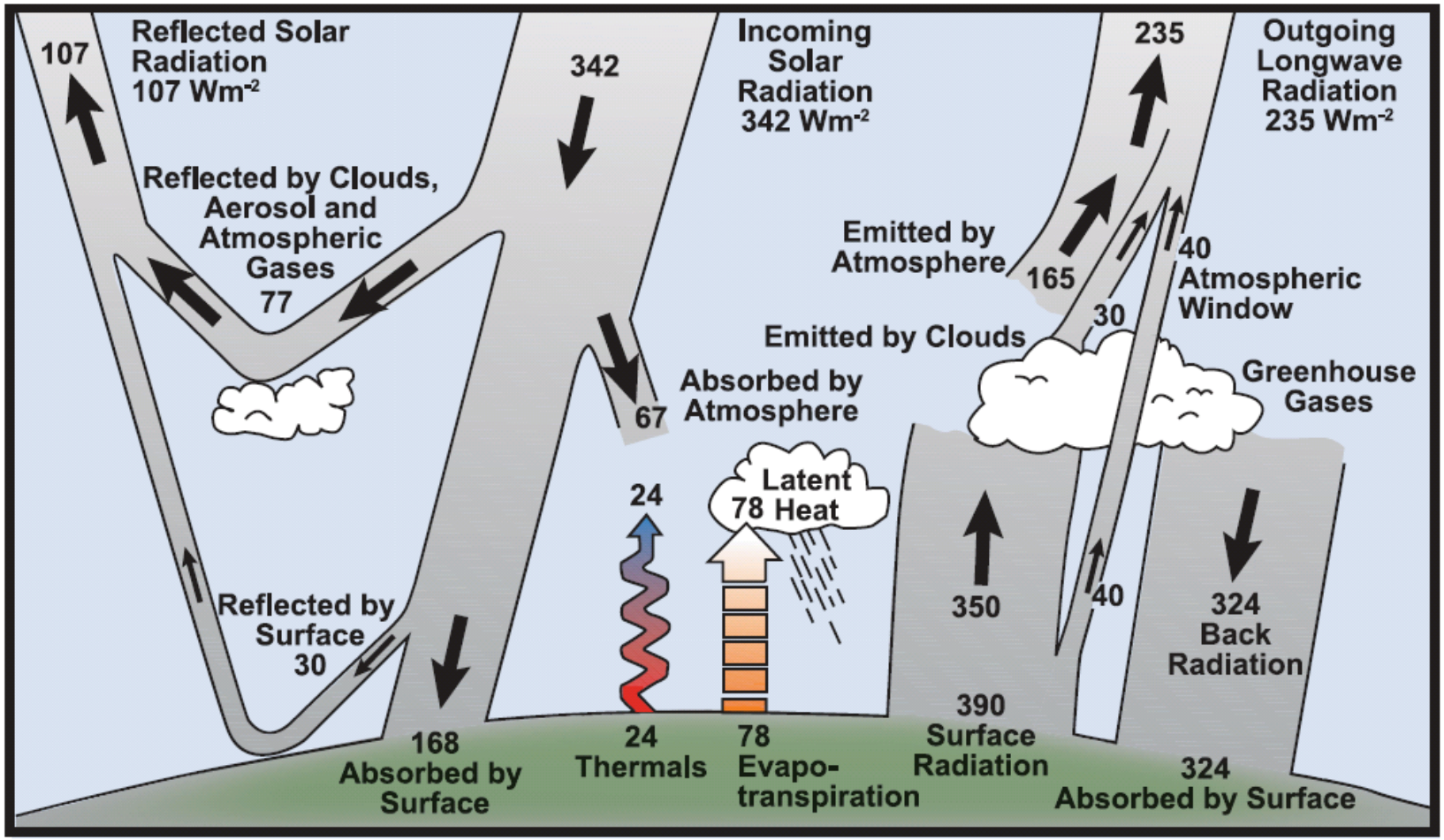

IPCC report, 2007

Cloud-aerosol interactions

- Twomey, 1977: High concentrations of aerosols reduce droplet size and increase cloud albedo for a constant amount of liquid water
- Albrecht, 1989: High aerosol concentrations narrow the size distribution, supressing precipitation and prolonging cloud lifetime
- aerosol-induced changes of cloud microstructure have profound impact on precipitation, dynamic evolution and vertical disposition of latent heat release (e.g. Rosenfeld, 2006)

Figure from Wallace and Hobbs

Cloud-aerosol interactions

- basic processes explaining cloud formation and evolution are well established
- but still many unresolved fundamental issues:
  - temporal and spatial evolution of clouds
  - lack of fundamental understanding of the glaciation of clouds
  - formation of rain in warm clouds
  - convective clouds

Impact of clouds on climate change

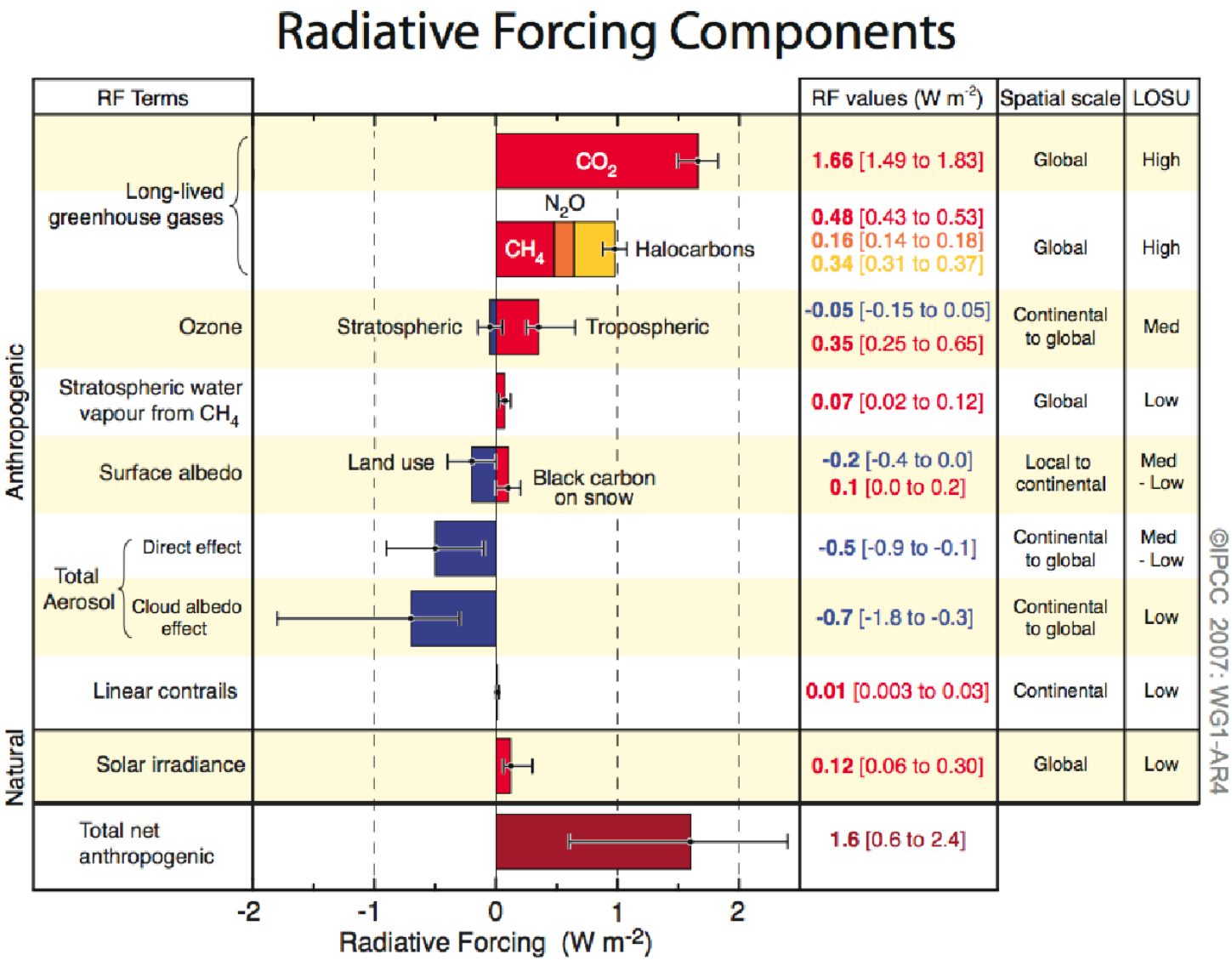

IPCC report 2007

IPCC Bericht 2007

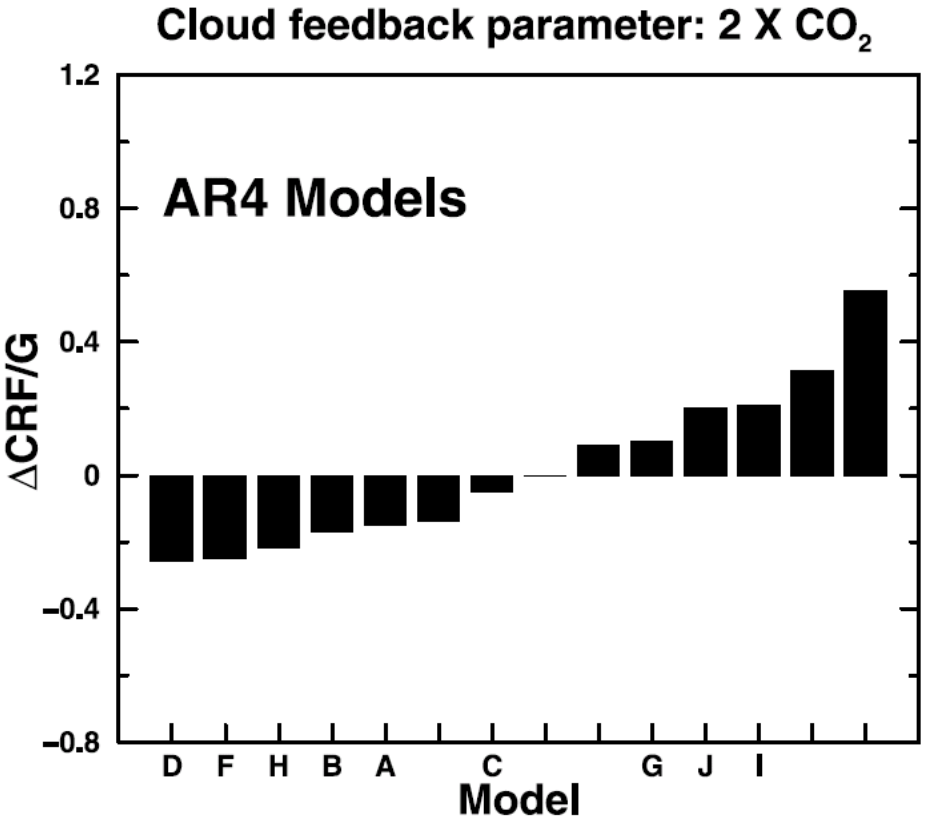

Ringer et al., GRL 2006

"Cloud feedbacks (particularly from low clouds) remain the largest source of uncertainty."

IPCC Report 2007, Technical Summary

Overview of cloud physics

- Atmospheric thermodynamics
  - gas laws, hydrostatic equation
  - 1st law of thermodynamics
  - moisture parameters
  - adiabatic / pseudoadiabatic processes
  - stability criteria / cloud formation
- Microphysics of warm clouds
  - nucleation of water vapor by condensation
  - growth of cloud droplets in warm clouds (condensation, fall speed of droplets, collection, coalescence)
  - formation of rain, stochastical coalescence
- Microphysics of cold clouds
  - homogeneous, heterogeneous, and contact nucleation
  - concentration of ice particles in clouds
  - crystal growth (from vapor phase, riming, aggregation)
  - formation of precipitation, cloud modification
- Observation of cloud microphysical properties
- (Parameterization of clouds in climate and NWP models)

Literature

John M. Wallace and Peter V. Hobbs. *Atmospheric Science, An introductory survey*. Elsevier, 2006.

R. R. Rogers. *A short course in cloud physics*. Pergamon Press, 1976.

Hans R. Pruppacher and James D. Klett. *Microphysics of clouds and precipitation*. Springer, 1996.

IPCC. Climate change 2007. Technical report, Intergovernmental Panel of Global Climate Change, 2007.

Additional publications and slides on website:
`http://www.meteo.physik.uni-muenchen.de/~emde/doku.php?id=teaching:cloud_microphysics:cloud_microphysics`

The ideal gas equation

- Equation of state: relation between p, V, T of a material
- Equation of state for gases $\Rightarrow$ ideal gas equation

$$pV = mRT \qquad p = \rho RT \qquad p\alpha = RT$$

- R - gas constant for 1 kg of gas
- $\alpha = 1/\rho$ - specific volume of gas (V occupied by 1 kg of gas at specific p and T)
- Boyle's law (T=const.) and Charles' laws (p=const., V=const.)

Sir Robort Boyle (1627–1691)

Jacques Charles (1746–1823)

Images from Wikipedia

Definitions

- gram-molecular weight (mole), e.g. 1 mol H_2O = 18.015 g
- number of moles $n = m/M$
- number of molecules in 1 mole N_A=6.022·10^{23} (Avogadro's number)
- Avogadro's hypothesis: gases containing the same number of molecules occupy the same volume
- universal gas constant R^*=8.3145JK^{-1}mol^{-1} $\Rightarrow pV = nR^*T$
- Boltzmann's constant k=R^*/N_A

Amedeo Avogadro (1776–1856)

Ludwig Boltzmann (1844–1906)

Images from Wikipedia

Adiabatic processes

adiabatic = change in physical state without heat exchange $\Rightarrow dq = 0$

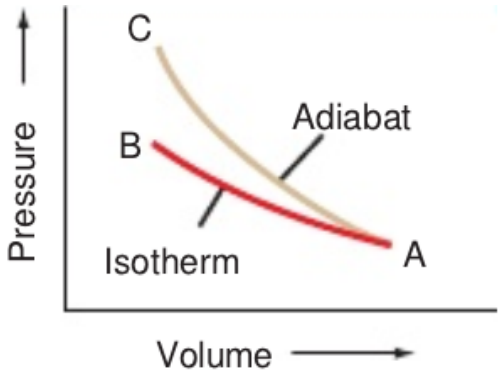

Fig. 3.5 An isotherm and an adiabat on a p–V diagram.
Figure from Wallace and Hobbs

$$dq = du + pd\alpha$$

T rises in adiabatic compression
T=const. in isothermal process

$$T_C > T_B \Rightarrow p_C > p_B$$

Concept of air parcel

Assumptions:

- *molecular mixing can be neglected* (in Earth's atmosphere only important above ≈105 km and for 1 cm layer above surface), i.e. mixing can be regarded as exchange of macroscale "air parcels"
- *parcel is thermally insulated from it's environment*, i.e.
  T changes adiabatically as parcel rises or sinks,
  p always adapts to environmental air, which is assumed to be in hydrostatic equilibrium
- *parcel moves slow enough*, i.e. the macroscopic kinetic energy is a negligible fraction of the total energy

Dry adiabatic lapse rate

for adiabatic processes:

$$d(c_p T + \phi) = 0 \Rightarrow -\frac{dT}{dz}_{\text{dry parcel}} = \frac{g}{c_p} \equiv \Gamma_d$$

Γ_d – dry adiabatic lapse rate (change of T with z)

Example for Earth's atmosphere:

- g=9.81 $\frac{m}{s^2}$, c_p=1004 $\frac{J}{K}$ $\Rightarrow \Gamma_d$=9.8 $\frac{K}{km}$
- Actual lapse rate (for moist air) is smaller than Γ_d.

Saturation vapor pressures

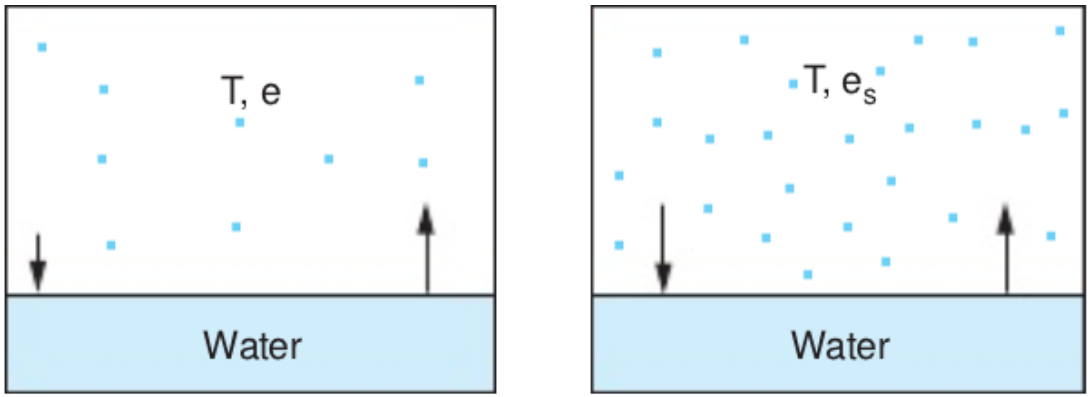

(a) Unsaturated (b) Saturated

Fig. 3.8 A box (a) unsaturated and (b) saturated with respect to a plane surface of pure water at temperature T. Dots represent water molecules. Lengths of the arrows represent the relative rates of evaporation and condensation. The saturated (i.e., equilibrium) vapor pressure over a plane surface of pure water at temperature T is e_s as indicated in (b).

Figure from Wallace and Hobbs

- equivalent definitions for water and ice

Saturation vapor pressure

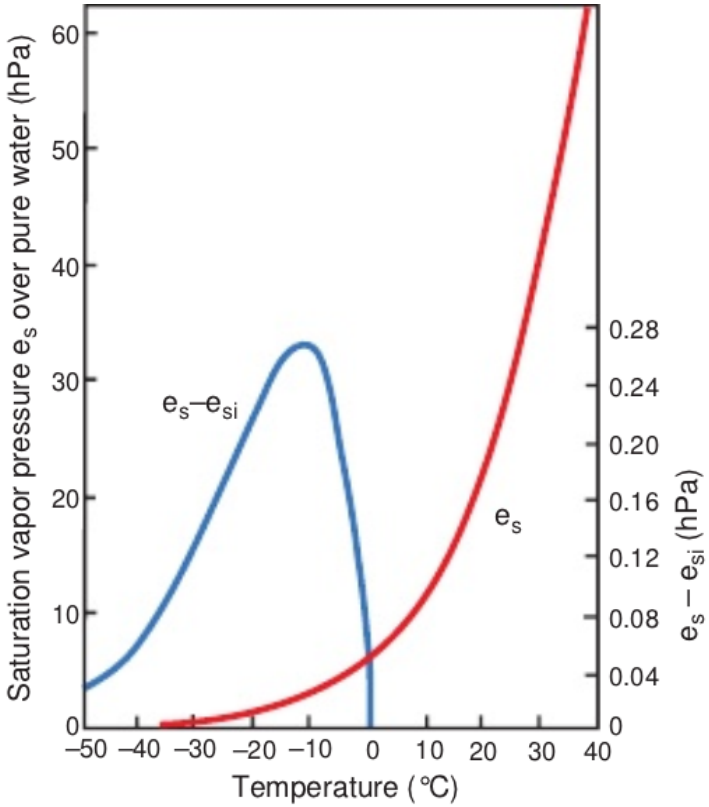

Fig. 3.9 Variations with temperature of the saturation (i.e., equilibrium) vapor pressure e_s over a plane surface of pure water (red line, scale at left) and the difference between e_s and the saturation vapor pressure over a plane surface of ice e_{si} (blue line, scale at right).

Figure from Wallace and Hobbs

- evaporation rate from ice less than from water : $e_s(T) > e_{si}(T)$

  $\Rightarrow$ ice particle in water-saturated air grows due to deposition of water vapor on it (important for formation of precipitation)

Saturation vapor pressure

Clausius-Clapayron equation

$$\frac{de_s}{dT} = \frac{L_v}{T(\alpha_v - \alpha_l)}$$

- integration yields $e_s(T)$, approximate because L_v depends on T

Magnus formula (empirical)

$$\text{water}(0°\text{C} - 100°\text{C}): \quad e_s = 6.1078 \exp\left(\frac{17.0809T}{234.175+T}\right)$$

$$\text{subcooled water}: \quad e_s = 6.1078 \exp\left(\frac{17.8436T}{245.425+T}\right)$$

$$\text{ice}: (-50°\text{C} - 0°\text{C}): \quad e_s = 6.1071 \exp\left(\frac{22.4429T}{272.44+T}\right)$$

T in °C and e_s in hPa.

Moisture parameters

- mixing ratio: $w = \frac{m_v}{m_d}$
  typically a few g/kg in mid-latitudes to 20 g/kg in tropics
- specific humidity: $q = \frac{m_v}{m_v+m_d} = \frac{w}{w+1}$
  w$\approx$0.01 $\rightarrow q \approx w$
- Saturation mixing ratio w_s:
  $w_s = \frac{m_{vs}}{m_d} = \cdots = \epsilon \frac{e_s}{p-e_s} \approx 0.622 \frac{e_s}{p}$ (since for atmospheric T: $p \gg e_s$)
- Relative humidity RH:
  $RH = 100 \frac{w}{w_s} = 100 \frac{e}{e_s}$ [%]
- Dew point T_D:
  temperature to which air must be cooled at p=const., so that air becomes saturated w.r.t. water (equivalent def. for frost point)

  measurement of T_D yields $RH = \frac{e_s(T_D,p)}{e_s(T,p)}$

Lifting condensation level (LCL)

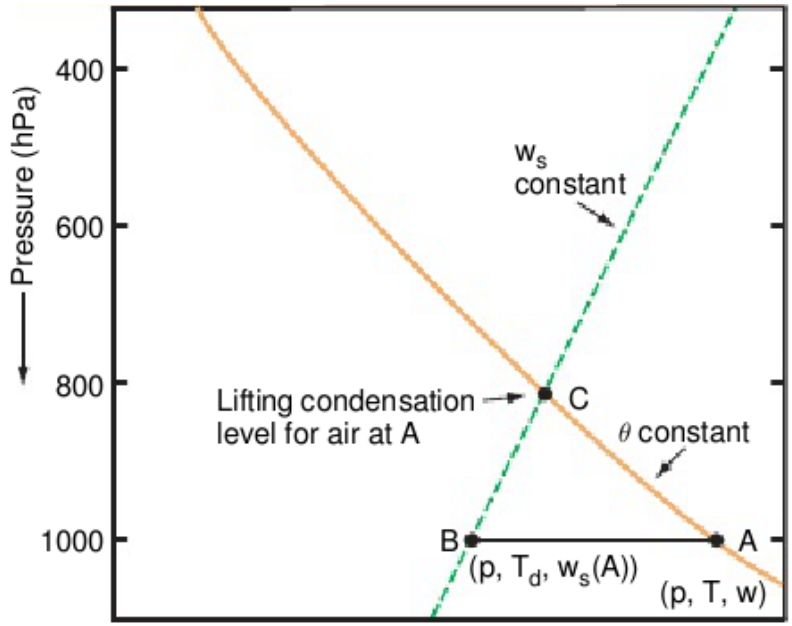

Fig. 3.10 The lifting condensation level of a parcel of air at A, with pressure p, temperature T, and dew point T_d, is at C on the skew $T - \ln p$ chart.

Figure from Wallace and Hobbs

- LCL: level to which moist air parcel can be lifted adiabatically before it becomes saturated w.r.t. water
- during lift: w=const., θ=const., w_s decreases until $w_s = w$ at LCL

Latent heats

- If heat is added to system $\Rightarrow$ change in T *or* change in phase
- phase transition: Δu completely used for changes in molecular configuration in presence of intermolecular forces

- Latent heat of melting L_m: heat that is required to convert unit mass of a material from solid to liquid phase without change in T, equal to latent heat of freezing
- melting point: T at which phase transition occurs
- for water at 1013hPa, 0°C $\Rightarrow L_m = 3.34 \cdot 10^5 \frac{J}{kg}$

- latent heat of vaporization or evaporation L_v defined equivalently
- for water 1013hPa, 100°C (boiling point) $\Rightarrow L_v = 2.25 \cdot 10^6 \frac{J}{kg}$

Saturated adiabatic and pseudoadiabatic processes

- air parcel rises $\Rightarrow$ T decreases with z until saturation is reached
- further lifting $\Rightarrow$ condensation of liquid water (or deposition on ice) $\Rightarrow$ release of latent heat $\Rightarrow$ rate of decrease in T reduced

Saturated adiabatic process

All condensation products remain in parcel, process still adiabatic and reversible

Pseudoadiabatic process

Condensation products fall out, process is irreversible. Not adiabatic since products carry out **small** amount of heat.

Saturated adiabatic lapse rate

$$\Gamma_s = -\frac{dT}{dz} \approx \frac{\Gamma_d}{1 + \frac{L_v}{c_p}\left(\frac{dw}{dT}\right)_p}$$

- Γ_s varies with p, T; in contrast to Γ
- since condensation releases heat: $\Gamma_s < \Gamma$

- typical values:
  4 K/km near ground in warm humid airmasses
  6-7 K/km in middle troposphere
  near tropopause, Γ_s only slightly smaller than Γ (e_s very small, no condensation)

Static stability for unsaturated air

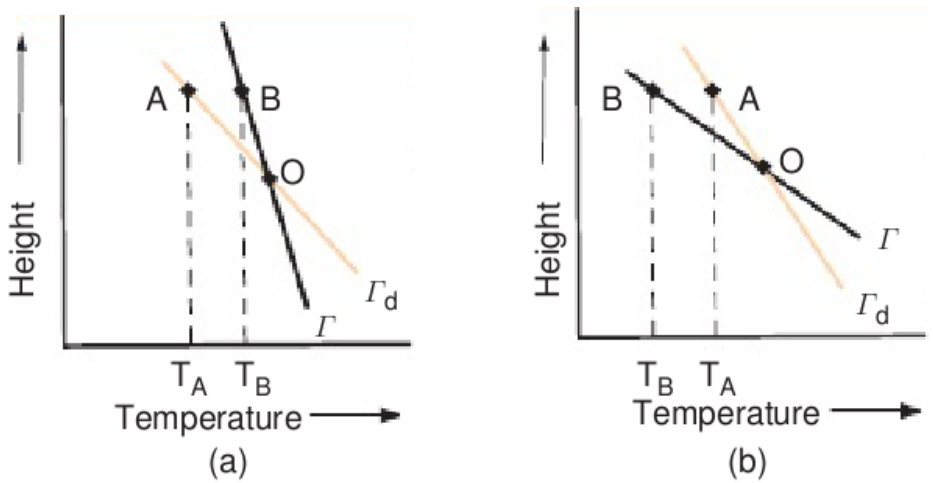

Fig. 3.12 Conditions for (a) positive static stability ($\Gamma < \Gamma_d$) and (b) negative static instability ($\Gamma > \Gamma_d$) for the displacement of unsaturated air parcels.

Figure from Wallace and Hobbs

- atmospheric layer with actual lapse rate Γ less than dry adiabatic lapse rate Γ_D $\Rightarrow$ stable stratification, positive static stability
- $\Gamma > \Gamma_D \Rightarrow$ unstable stratification, positive static stability (not persistant in free atmosphere due to strong vertical mixing)
- $\Gamma = \Gamma_D \Rightarrow$ neutral
- Same for saturated air, when Γ_S is used instead of Γ_D

Gravity waves

For stably stratified layers, so called gravity waves may form.

buoyancy oscillation of air parcel

$$z'(t) = z'(0)\cos Nt$$

Brunt-Väisälä frequency

$$N = \left(\frac{g}{T}\left(\Gamma_d - \Gamma\right)\right)^{1/2}$$

Gravity waves

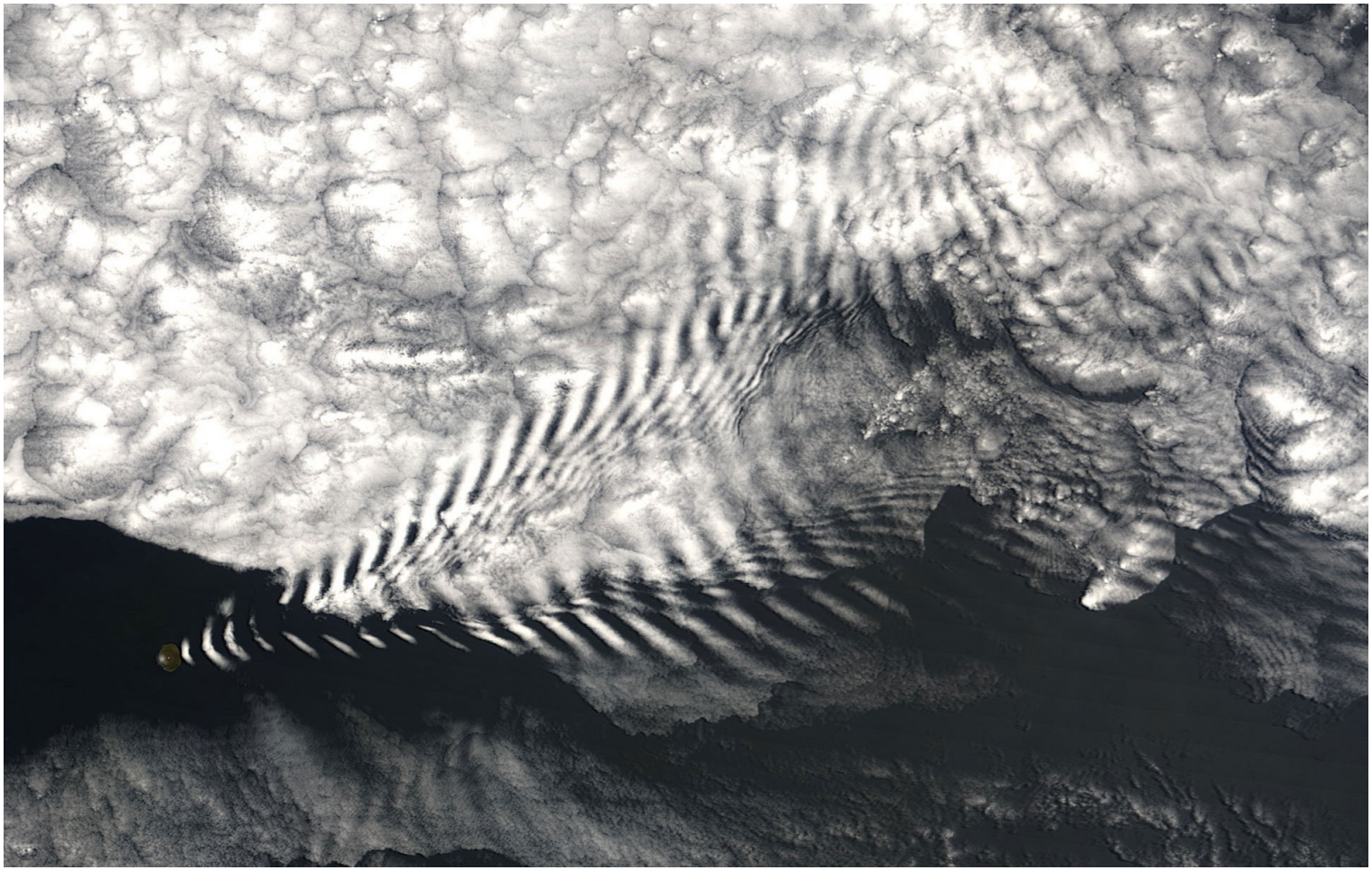

from Wikipedia

Conditional and convective stability

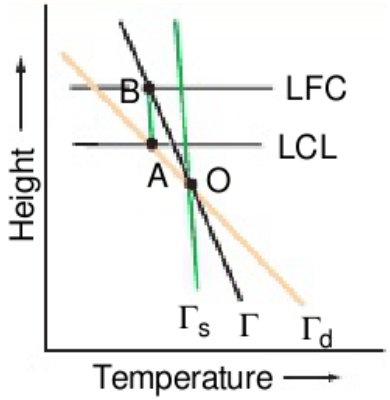

Fig. 3.16 Conditions for conditional instability ($\Gamma_s < \Gamma < \Gamma_d$). Γ_s and Γ_d are the saturated and dry adiabatic lapse rates, and Γ is the lapse rate of temperature of the ambient air. LCL and LFC denote the *lifting condensation level* and the *level of free convection*, respectively.

Figure from Wallace and Hobbs

- atmospheric layer with actual lapse rate between Γ_S and Γ_D $\Rightarrow$ conditional instability
- Level of free convection (LFC) $\Rightarrow$ from this level parcel is unstable, is carried upward in absence of forced lifting
- vigorous convective overturning can occur if vertical motions are large enough to lift air parcel beyond LFC

Phase transitions

vapor	$\leftrightarrow$ liquid	condensation, evaporation
liquid	$\leftrightarrow$ solid	freezing, melting
vapor	$\leftrightarrow$ solid	deposition, sublimation

Changes from left to right:

$\Rightarrow$ increasing molecular order, “free energy barrier” to overcome
$\Rightarrow$ cloud forming processes

saturation = equilibrium condition for thermodynamic system consisting of vapor (ice) and liquid

Why do droplets form?

- at equilibrium (saturation):
  rate of condensation = rate of evaporation
- energy barrier of small droplets: generally no phase transition at saturation (homogeneous nucleation unlikely)
- when air parcels ascent without condensation $\Rightarrow$ supersaturation
- energy barrier may be decreased by cloud condensation nuclei $\Rightarrow$ heterogeneous nucleation
  - hygroscopic particles serve as centers of condensation
  - supersaturation in clouds not much larger than 1%
- when air parcel including cloud droplets ascend to $T<0°$
  - droplets become supercooled
  - freeze when ice nuclei are present

Energy difference due to formation of droplet

ΔE = surface energy of droplet - Gibbs free energy due to condensation

$$\Delta E = 4\pi R^2 \sigma - \frac{4}{3}\pi R^3 nkT \ln \frac{e}{e_s}$$

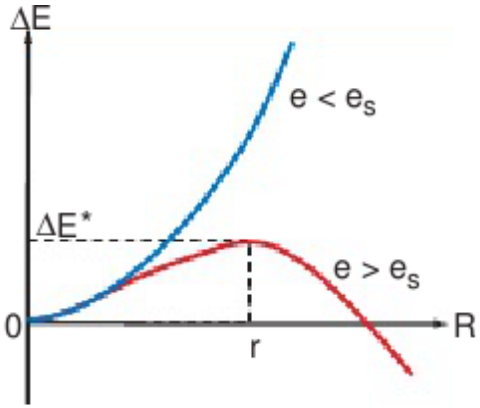

Fig. 6.1 Increase ΔE in the energy of a system due to the formation of a water droplet of radius R from water vapor with pressure e; e_s is the saturation vapor pressure with respect to a plane surface of water at the temperature of the system.
Figure from Wallace and Hobbs

- blue curve: subsaturated conditions, formation of droplets not possible
- red curve: supersaturated conditions, droplets grow above radius r

Energy difference due to formation of droplet

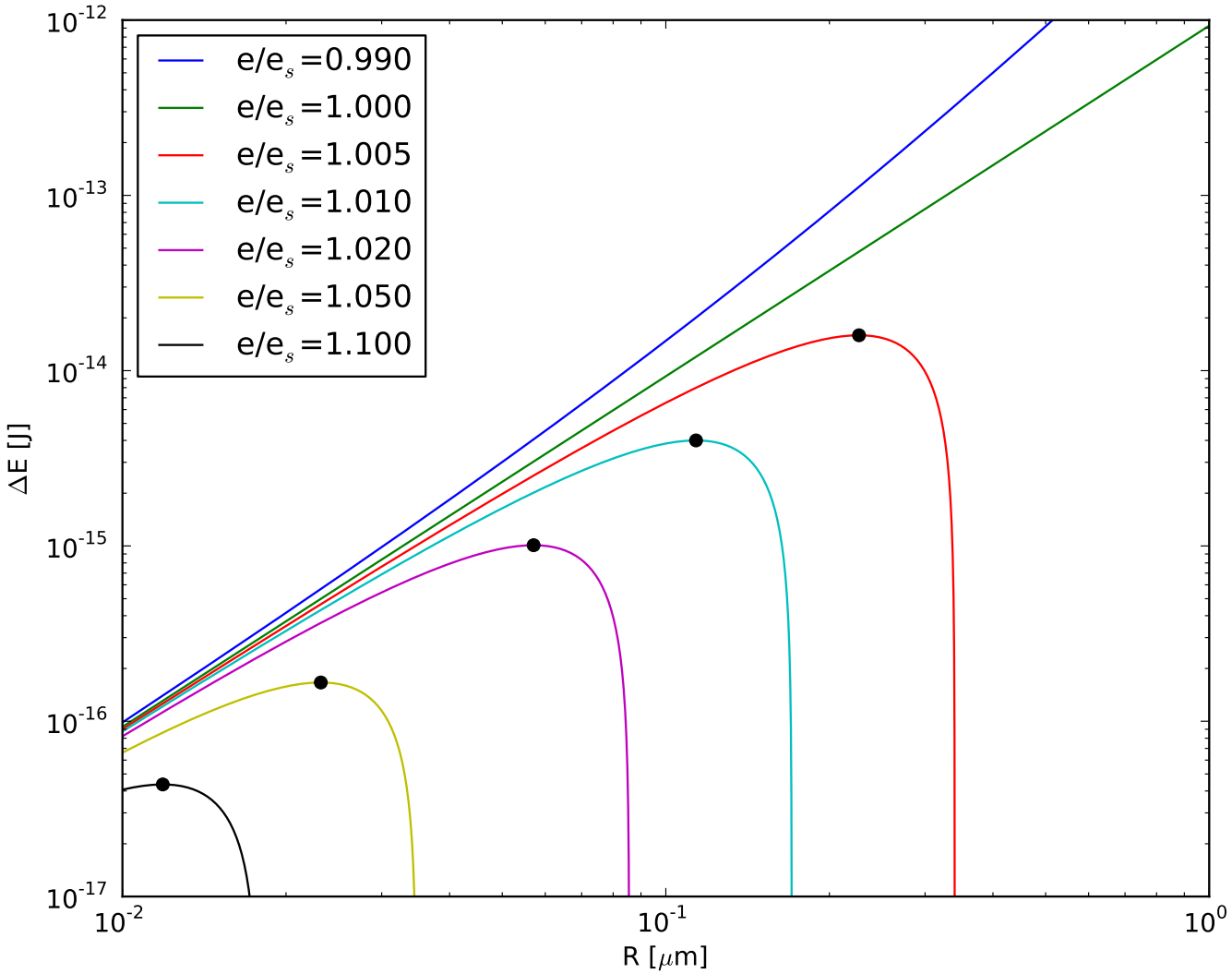

Kelvin equation

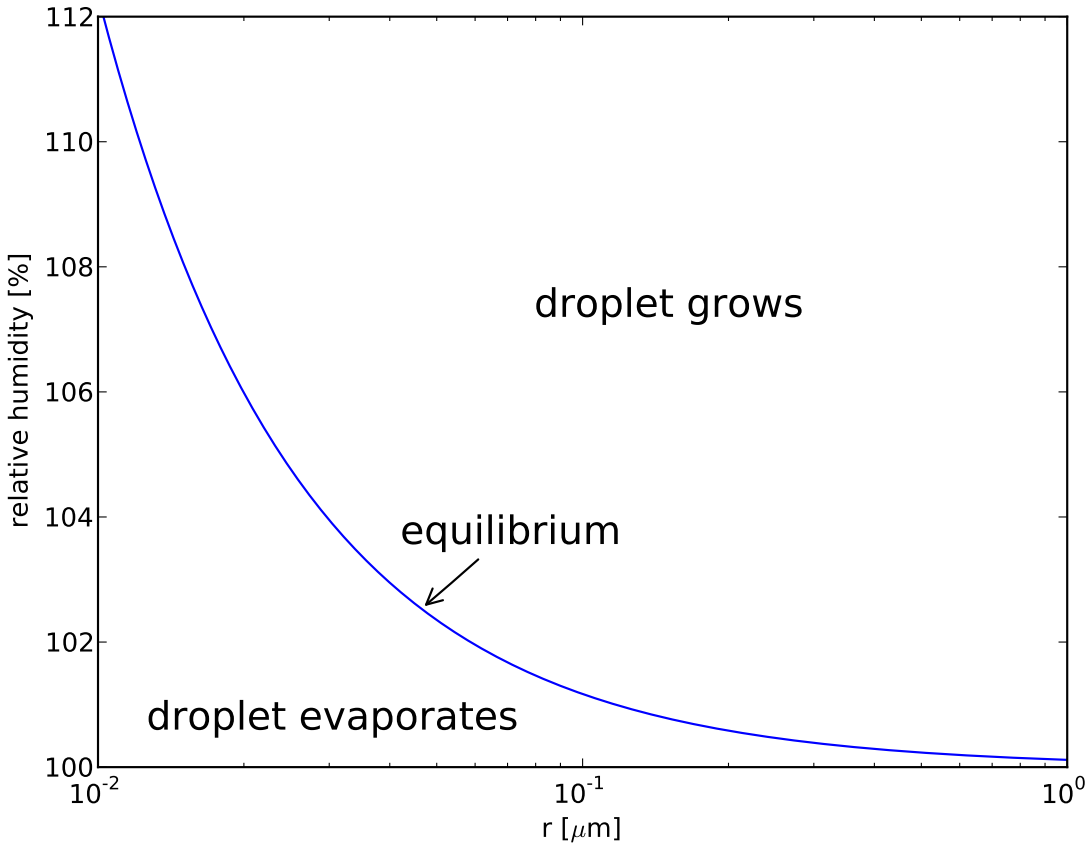

Kelvin equation

$$r = \frac{2\sigma}{nkT \ln \frac{e}{e_s}}$$

Heterogeneous nucleation

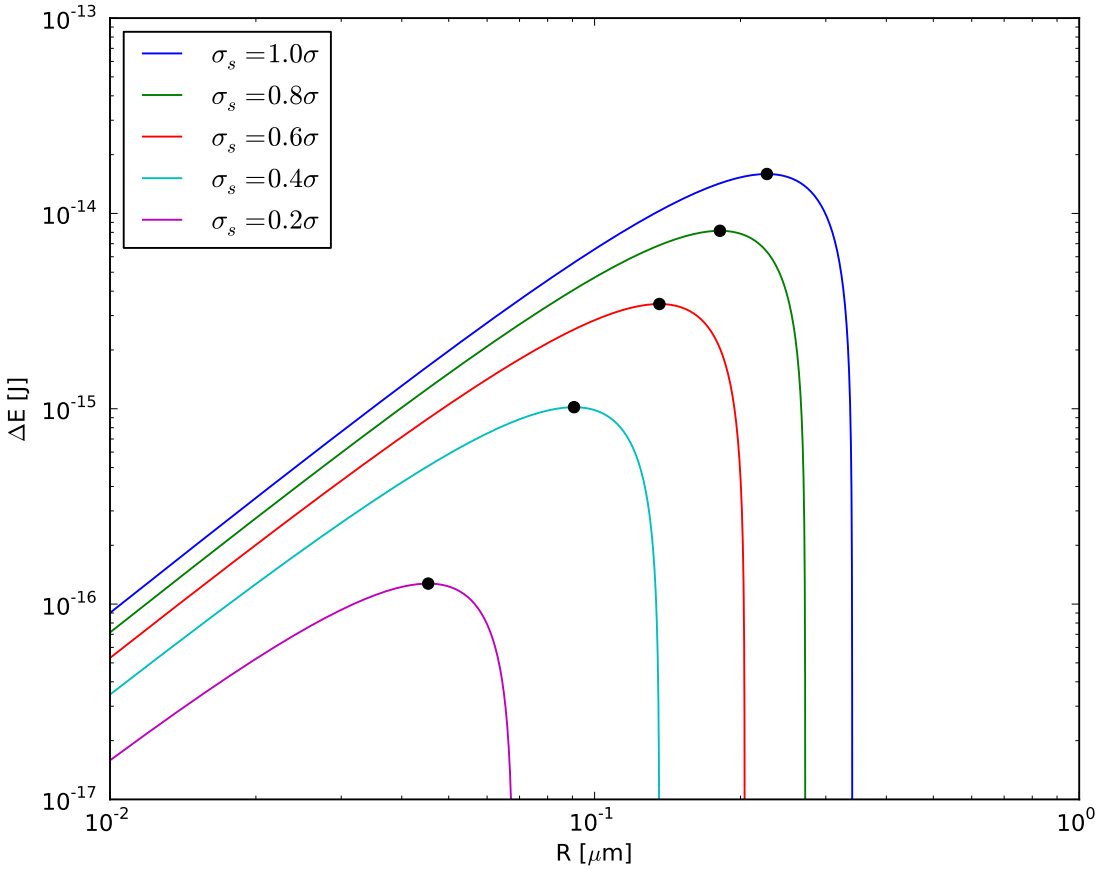

Surface tension is reduced when soluble aerosol is added to droplet.

Calculation for 0.5% supersaturation, T=293 K.

Raoult's law

Vapor pressure of an ideal solution depends on mole fraction of the component present in the solution

$$\frac{e'}{e} = f$$

- e' – saturation water vapor pressure adjacent to solution droplet containing a mole fraction f of pure water
- e – saturation water vapor pressure adjacent to pure water droplet
- f – number of moles of pure water devided by total number of moles

$\Rightarrow$ saturation water vapor pressure is reduced when aerosol is solved in droplet

Köhler curves

$$\frac{e}{e_s} = \left(\exp \frac{2\sigma'}{n' k T r}\right)\left(1 + \frac{imM_w}{M_s\left(\frac{4}{3}\pi r^3 \rho' - m\right)}\right)^{-1}$$

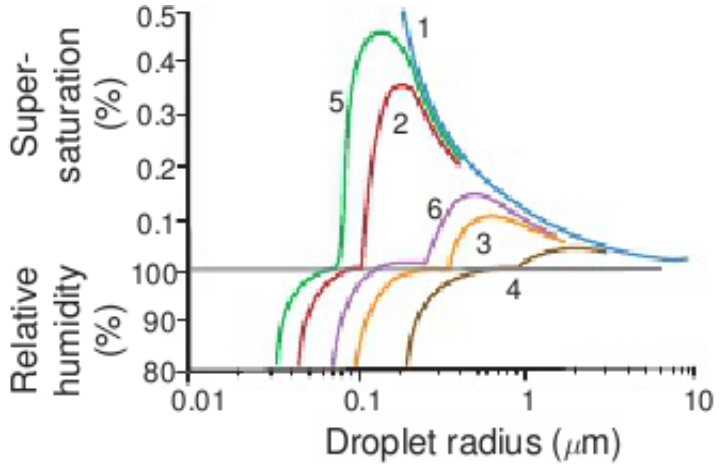

Fig. 6.3 Variations of the relative humidity and supersaturation adjacent to droplets of (1) pure water (blue) and adjacent to solution droplets containing the following fixed masses of salt: (2) 10^{-19} kg of NaCl, (3) 10^{-18} kg of NaCl, (4) 10^{-17} kg of NaCl, (5) 10^{-19} kg of $(NH_4)_2SO_4$, and (6) 10^{-18} kg of $(NH_4)_2SO_4$. Note the discontinuity in the ordinate at 100% relative humidity. [Adapted from H. R. Pruppacher, "The role

Figure from Wallace and Hobbs

Droplet activation

Droplets grow along Köhler curve

- Case 1: when ambient supersaturation is higher than maximum
  $\Rightarrow$ activated droplets
- Case 2: when ambient supersaturation is lower than maximum, droplets grow to equilibrium state, where ambient supersaturation equals supersaturation adjacent to droplet
  $\Rightarrow$ unactivated/haze droplets

Efficiency of cloud condensation nuclei

- small subset of atmospheric aerosols serve as CCN
- CCN are most efficient when droplets can grow at supersaturations as low as possible
  - the larger the size the lower the required supersaturation
  - the greater the solubility the lower the required supersaturation

Growth of droplets in warm clouds

1. Growth by condensation

2. Growth by collision and coalescene

Droplet growth by condensation

- air parcel rises, expands, cools adiabatically and reaches saturation
- further lifting produces supersaturation
- as supersaturation rises, CCN are activated (most efficient first)
- supersaturation reaches maximum when:

rate of water vapor in excess of saturation made available by adiabatic cooling	=	rate of water vapor which condenses on CCN and droplets
concentration of cloud droplets	=	concentration of CCN activated by attained peak supersaturation

Growth rate and size distribution

- growing droplets consume water vapor faster than it is made availabe by cooling and supersaturation decreases
- haze droplets evaporate, activated droplets continue to grow by condensation

growth rate of water droplet

$$\frac{dr}{dt} = G_I S \frac{1}{r}$$

- smaller droplets grow faster than larger droplets
- sizes of droplets in cloud become increasingly uniform, approach monodispersed distribution

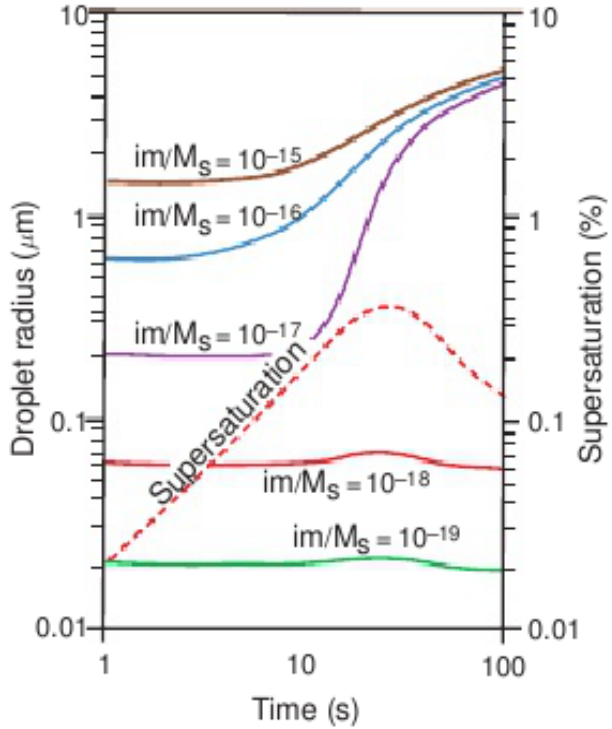

Fig. 6.16 Theoretical computations of the growth of cloud condensation nuclei by condensation in a parcel of air rising with a speed of 60 cm s^{-1}. A total of 500 CCN cm^{-1} was assumed with im/M_s values [see Eq. (6.8)] as indicated. Note how the droplets that have been activated (brown, blue, and purple curves) approach a monodispersed size distribution after just 100 s. The variation with time of the supersaturation of the air parcel is also shown (dashed red line). [Based on data from *J. Meteor.* **6**, 143 (1949).]

Figure from Wallace and Hobbs

Sizes of cloud droplets

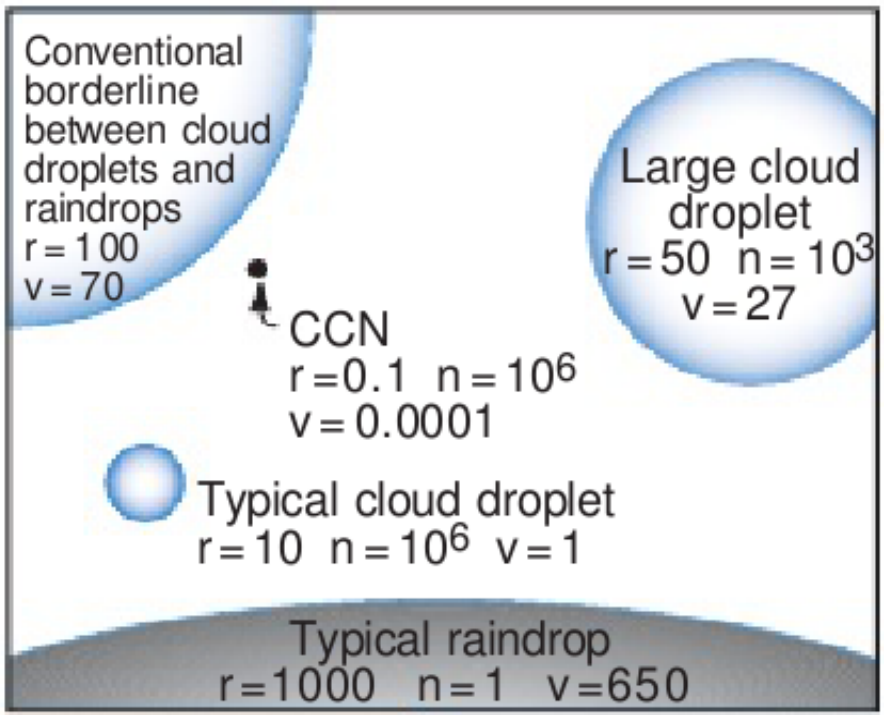

Figure from Wallace and Hobbs

- growth by condensation alone can not produce raindrops with radii of several mm !

Collision efficiency

Collision efficiency

$$E = \frac{y^2}{r_1^2 + r_2^2}$$

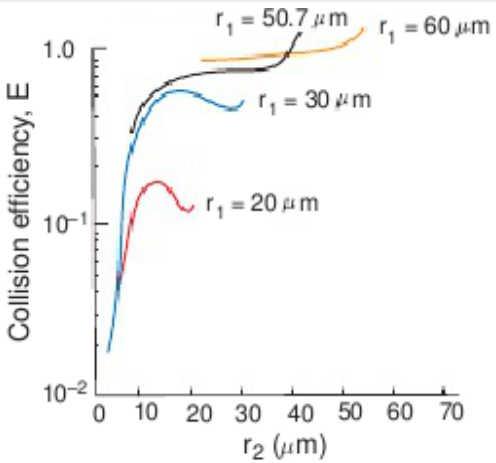

Fig. 6.20 Calculated values of the collision efficiency, E, for collector drops of radius r_1 with droplets of radius r_2. [Adapted from H. R. Pruppacher and J. D. Klett, *Microphysics of Clouds and Precipitation*, Kluwer Academic Pub., 1997, Fig. 14-6, p. 584, Copyright 1997, with kind permission of Springer Science and Business Media. Based on *J. Atmos. Sci.* **30**, 112 (1973).]

Figure from Wallace and Hobbs

- E increases when size of collector drop r_1 increases
- E small for $r_1 < 20\mu$m
- $r_1 \gg r_2$: E small because small droplets follow streamlines around collector drop
- E increases with increasing r_2 until $r_2/r_1 \approx 0.6$–0.9
- $r_2/r_1 >$0.6–0.9: E decreases because relative velocity between droplets becomes small
- $r_2/r_1 \approx$1: strong interaction between droplets, E increases again

Coalescence

Coalescence: Droplet is captured when it collides with larger droplet

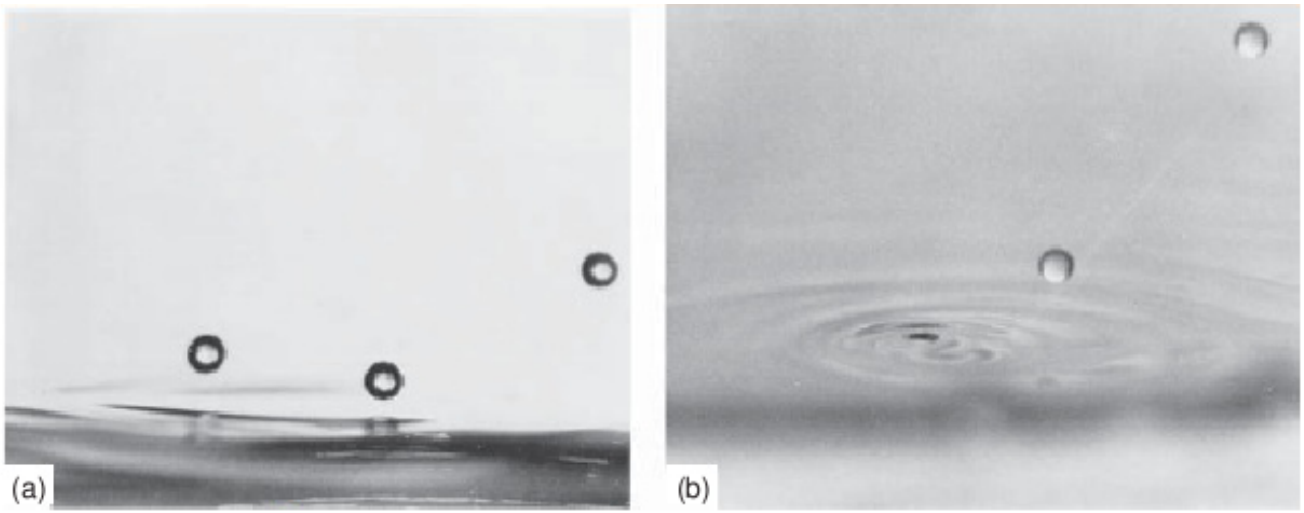

Fig. 6.21 (a) A stream of water droplets (entering from the right), about 100 μm in diameter, rebounding from a plane surface of water. (b) When the angle between the stream of droplets and the surface of the water is increased beyond a critical value, the droplets coalesce with the water. [Photograph courtesy of P. V. Hobbs.]

Figure from Wallace and Hobbs

Coalescence efficiency

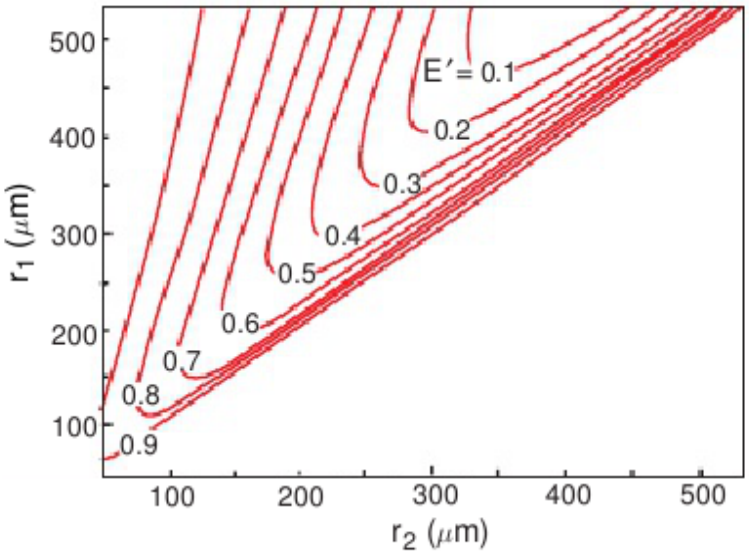

Fig. 6.22 Coalescence efficiencies E' for droplets of radius r_2 with collector drops of radius r_1 based on an empirical fit to laboratory measurements. [Adapted from *J. Atmos. Sci.* **52**, 3985 (1995).]

Figure from Wallace and Hobbs

Coalescence efficiency

E'=fraction of collisions that result in coalescence

- E' large for $r_2 \ll r_1$
- E' initially decreases as r_2 increases
- as r_2 approaches r_1, E' increases sharply

Collection efficiency

$$E_c = E \cdot E'$$

Continuous collection model

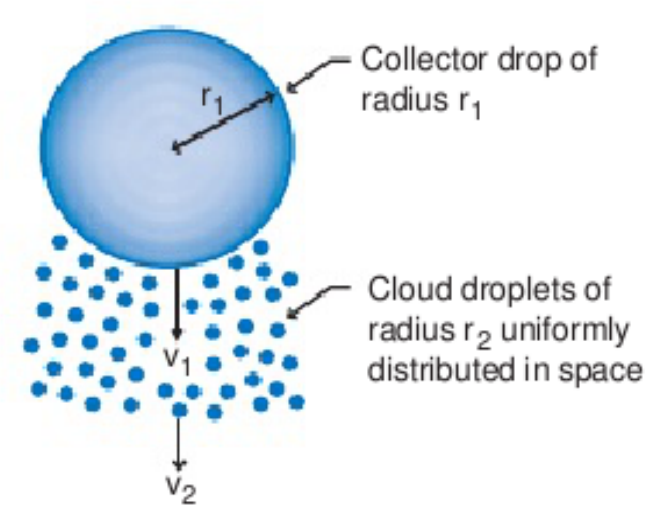

Fig. 6.23 Schematic illustrating the continuous collection model for the growth of a cloud drop by collisions and coalescence.

Figure from Wallace and Hobbs

- collector drop with radius r_1 and terminal velocity v_1
- drop falls in still air through cloud of equal sized droplets with r_2 and v_2
- droplets are uniformly distributed and collected uniformly by all collector drops of a given size

Gap between condensational and collectional growth

- condensational growth
  - slows appreciably as droplet radius approaches $\sim 10\mu$m
  - tends to produce monodisperse size distribution
  - droplets then have similar fall speeds $\Rightarrow$ collisions become unlikely
- collectional growth
  - conditions: a few reasonably efficient collector drops (i.e. r$>$ 20μm) cloud deep enough and contains sufficient amount of water
- Question 1: How do the collector drops initially form

Broad size distributions

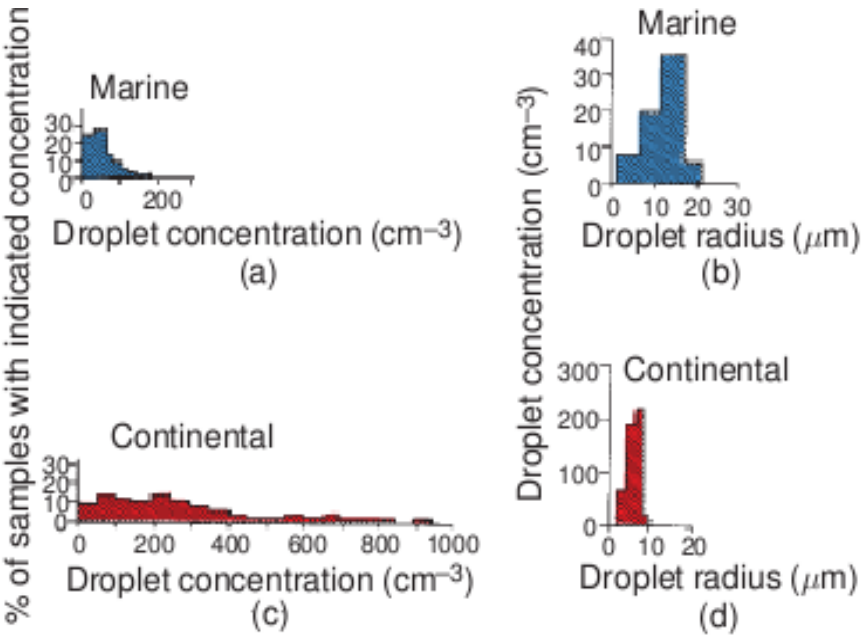

Fig. 6.7 (a) Percentage of marine cumulus clouds with indicated droplet concentrations. (b) Droplet size distributions in a marine cumulus cloud. (c) Percentage of continental cumulus clouds with indicated droplet concentrations. (d) Droplet size distributions in a continental cumulus cloud. Note change in ordinate from (b). [Adapted from P. Squires, "The microstructure and colloidal stability of warm clouds. Part I—The relation between structure and stability," *Tellus* **10**, 258 (1958). Permission from Blackwell Publishing Ltd.]

Figure from Wallace and Hobbs

Question 2:
How do the broad size distributions form that are commonly measured?

Possible answers

- Giant cloud condensation nuclei (GCCN)
- Turbulence (enhances collision efficiency, fluctuations in supersaturation
- Radiative broadening (droplet loses heat, saturation vapor pressure lower, faster growth)
- Stochastic collection

Shape of raindrops

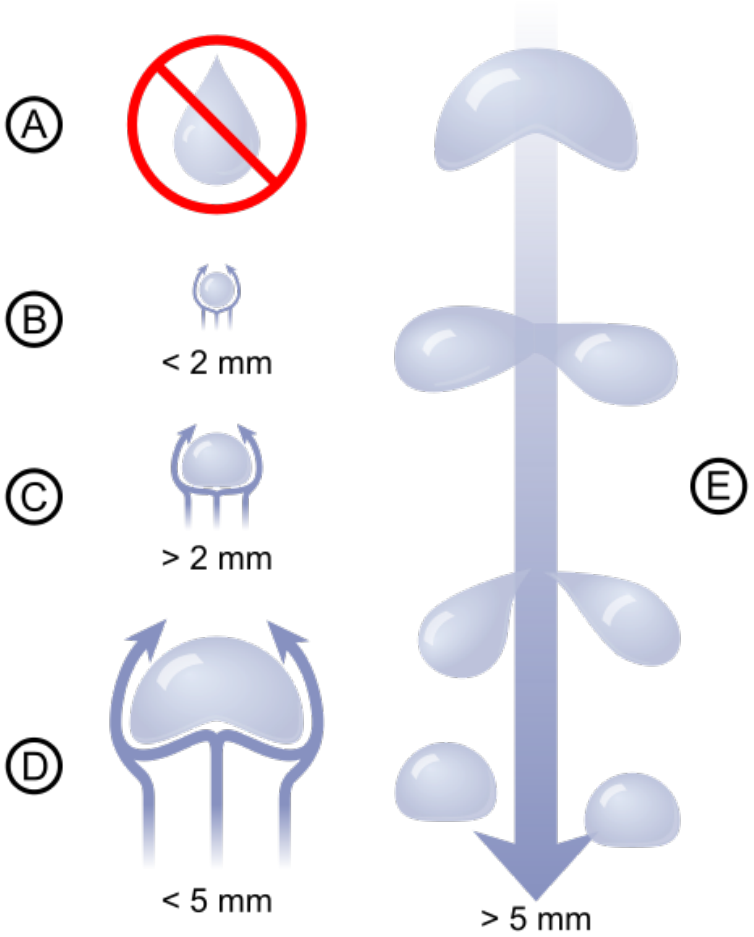

Figure from Wikipedia

- as raindrop size increases it becomes flattened, gradually changes shape from spherical to increasingly parachute
- if initial radius $>$ 2.5mm parachute becomes inverted bag with toroidal ring of water around lower rim
- when drop bursts to produce fine spray of droplets, toroidal ring breaks up into large drops

Size distribution of raindrops

Measurements of the size distribution of raindrops that reach the ground can often be fitted to the same size distribution function:

Marshall-Palmer distribution

$$N(D) = N_0 \exp -\Lambda D$$

$N(D)dD$ – number of drops per unit volume with diameters between D and $D + dD$
N_0 and Λ – empirical fitting parameters

N_0 almost const., Λ varies with rainfall rate

Microphysics of cold clouds

- cold cloud: cloud that extends above 0°C level
- mixed cloud: clouds containing liquid droplets and ice crystals
- glaciated cloud: pure ice cloud

Homogeneous nucleation

- water droplets become super-cooled when air parcel ascends and cools down
- homogeneous nucleation: pure water droplet freezes
  phase transition: liquid $\Rightarrow$solid
- process analogue to nucleation of liquid droplet from vapor phase

Homogeneous and heterogeneous nucleation

- measured median freezing temperatures
- homogeneous freezing
- heterogeneous freezing

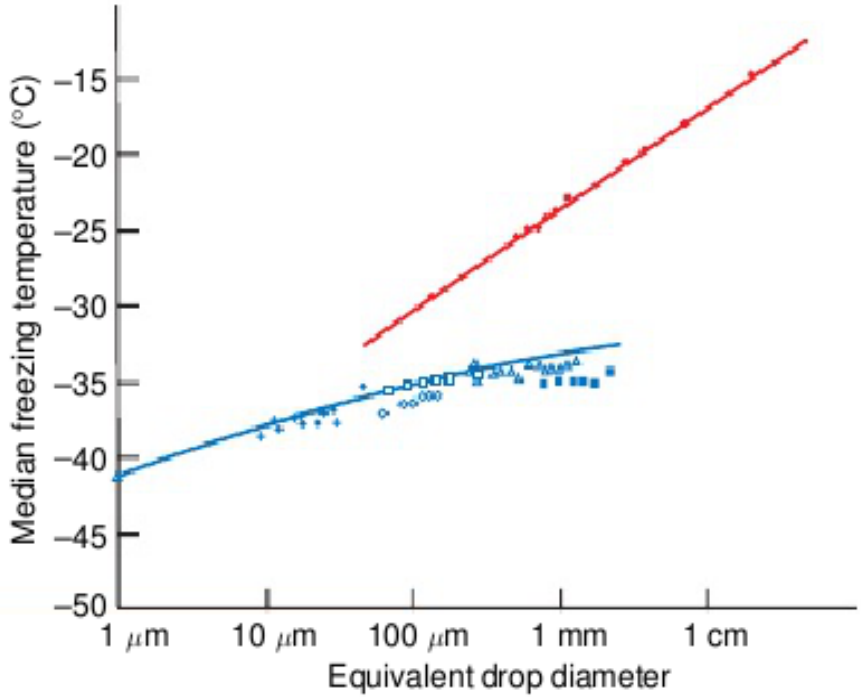

Fig. 6.29 Median freezing temperatures of water samples as a function of their equivalent drop diameter. The different symbols are results from different workers. The red symbols and red line represent heterogeneous freezing, and the blue symbols and line represent homogeneous freezing. [Adapted from B. J. Mason, *The Physics of Clouds*, Oxford Univ. Press, Oxford, 1971, p. 160. By permission of Oxford University Press.]

Figure from Wallace and Hobbs

Heterogeneous nucleation

- water molecules in droplet collect onto surface of particle contained in droplet (freezing nucleus) ⇒ice like structure is formed ⇒growth starts at larger crystal size ⇒freezing occurs
- heterogeneous nucleation occurs at much higher T than homogeneous nucleation

Ice nucleating crystals

crystal substance	lattice constants [Å] a	b	reported nucleation threshold [°C]
Ice	4.52	7.37	
AgI	4.58	7.49	-4
PbI_2	4.54	6.86	-6

Table: adapted from Byers, Elements of cloud physics

AgI and PbI_2 have hexagonal structures and are insoluble in water

The lattice structure is very similar to ice $\Rightarrow$AgI and PbI_2 are active nucleation agents for ice crystals

Further nucleation processes

Contact nucleation

Freezing starts when suitable particle (contact nucleus) comes into contact with super-cooled droplet.

Deposition

Some particles (deposition nuclei) serve as centers where ice forms directly from vapor phase. Conditions: air supersaturated w.r.t. ice and T sufficiently low

When air is supersaturated w.r.t. ice and water, some particles may act as freezing nucleus (vapor $\Rightarrow$liquid $\Rightarrow$ice) or as deposition nucleus (vapor $\Rightarrow$ice).

Onset of ice nucleation

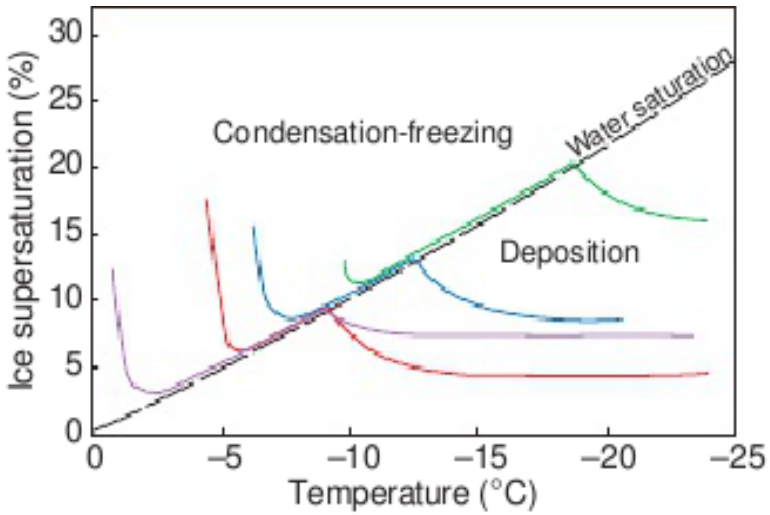

Fig. 6.30 Onset of ice nucleation as a function of temperature and supersaturation for various compounds. Conditions for condensation-freezing and ice deposition are indicated. Ice nucleation starts above the indicated lines. The materials are silver iodide (red), lead iodide (blue), methaldehyde (violet), and kaolinite (green). [Adapted from *J. Atmos. Sci.* **36**, 1797 (1979).]

Figure from Wallace and Hobbs

- Onset of of ice nucleation as function of temperature and supersaturation
- Onset occurs at higher T under water-supersaturated conditions
- Lower T required under water-subsaturated conditions, when only deposition is possible

Measurements of ice nucleus concentrations

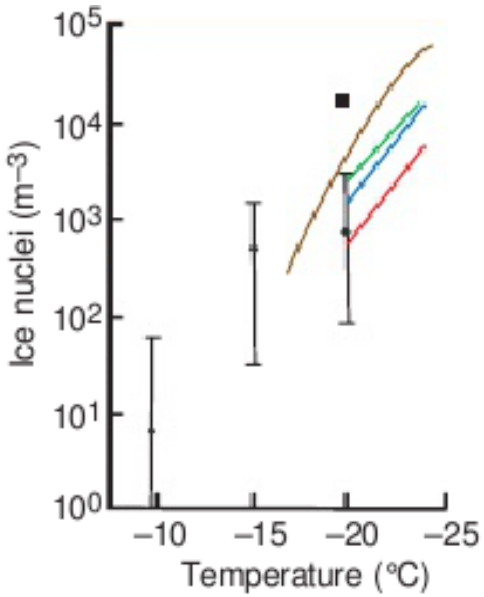

Fig. 6.31 Measurements of average ice nucleus concentrations at close to water saturation in the northern and southern hemispheres. Southern hemisphere, expansion chamber (red); southern hemisphere, mixing chamber (blue); northern hemisphere, expansion chamber (green); northern hemisphere, mixing chamber (black square); Antarctica, mixing chamber (brown). Vertical lines show the range and mean values (dots) of ice nucleus concentrations based on Millipore filter measurements in many locations around the world.

Figure from Wallace and Hobbs

Empirical relationship

$$\ln N = a(T - T_1)$$

T_1 – temperature at which 1 nucleus/liter is active (typically $\approx 20°C$)
a – constant between 0.3 and 0.6, depending on conditions

e.g. a=0.6 $\Rightarrow$N increases by factor of 10 for every 4°decrease in T

Effect of supersaturation on ice nucleus concentration

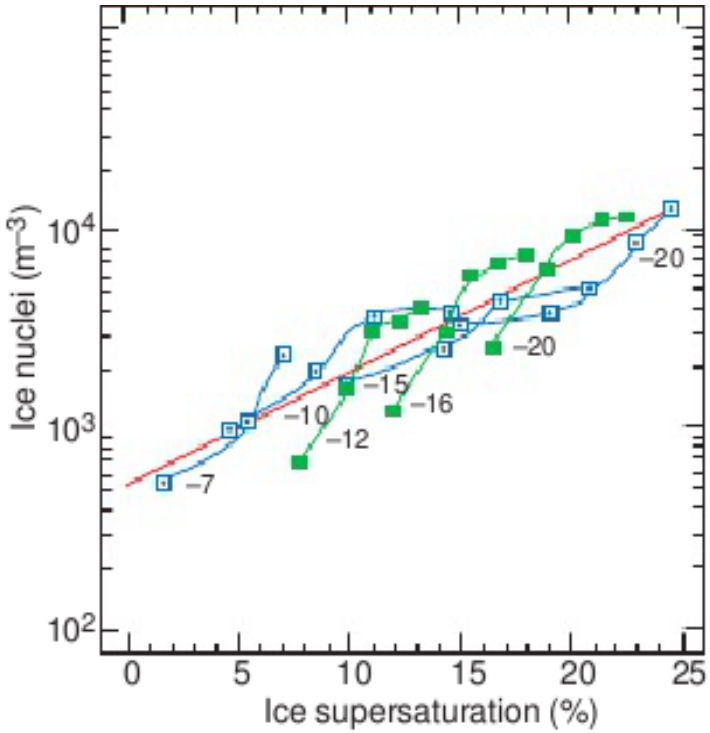

Fig. 6.32 Ice nucleus concentration measurements versus ice supersaturation; temperatures are noted alongside each line. The red line is Eq. (6.35). [Data reprinted from D. C. Rogers, "Measurements of natural ice nuclei with a continuous flow diffusion chamber," *Atmos. Res.* **29**, 209 (1993) with permission from Elsevier—blue squares, and R. Al-Naimi and C. P. R. Saunders, "Measurements of natural deposition and condensation-freezing ice nuclei with a continuous flow chamber," *Atmos. Environ.* **19**

The greater the supersaturation the more particles act as ice nuclei.

empirical fit:

$$N = \exp(a + b(100(S_i - 1)))$$

a=-0.639, b=0.1296

Maximum concentration of ice particles

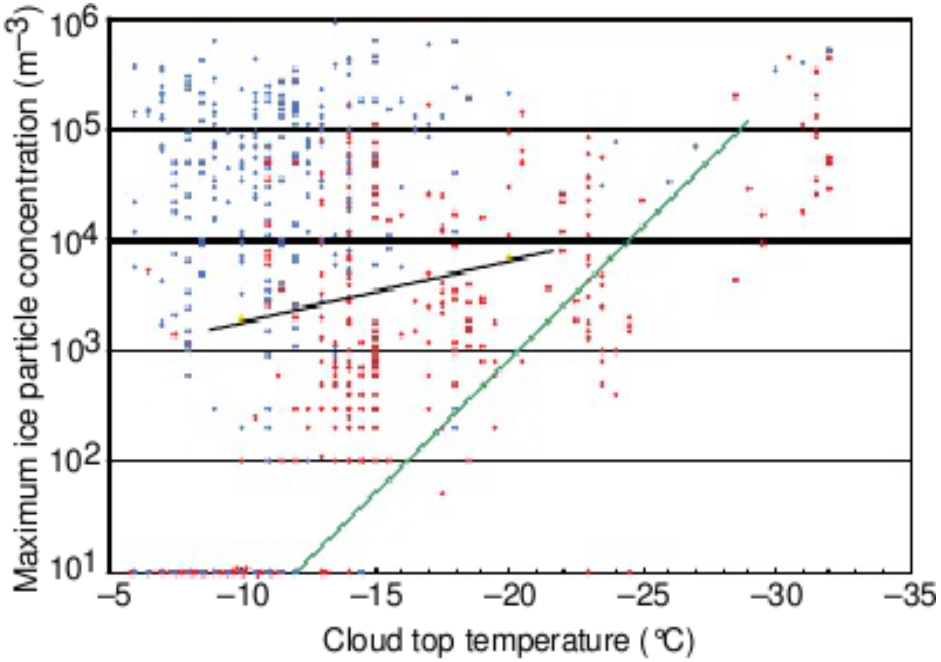

Fig. 6.34 Maximum concentrations of ice particles versus cloud top temperature in mature and aging marine cumuliform clouds (blue dots) and in continental cumuliform clouds (red dots). Note that on the abscissa temperatures decrease to the right. Symbols along the abscissa indicate ice concentrations ≤ 1 liter^{-1}, which was the lower limit of detection. The green line shows ice nucleus concentrations predicted by Eq. (6.33) with $a = 0.6$ and $T_1 = 253$ K. The black line shows ice nucleus concentrations from (6.35) assuming water-saturated conditions. [Data from *J. Atmos. Sci.* **42**, 2528 (1985); and *Quart. J. Roy. Met. Soc.* **117**, 207 (1991) and **120**, 573 (1994). Repro-

- empirical relation from laboratory measurements corresponds to minimum values of maximum concentrations
- concentrations in natural clouds can be several orders of magnitude larger !

Explanations for high ice crystal concentrations

- measurement techniques in laboratory can not be applied to natural clouds (conditions too different)
- ice multiplication or ice enhancement process
  - some crystals are fragile and may break up in several splinters when colliding with other particles
  - Super-cooled droplet freezes in isolation (e.g. free fall), or after it collides with an ice particle (i.e. riming – freezing of droplet on ice crystal) $\Rightarrow$freezing in 2 stages, particle may explode in 2nd stage of freezing

Riming

Riming

Freezing of droplet on ice crystal.

- riming might be most important for ice enhancement
- when ice particle falls through super-cooled cloud it is impacted by thousands of droplets, each may shed numerous ice splinters
- Laboratory measurement
  - Setup:
    - droplet concentration: 50/cm^3
    - droplet diameter: 5–35μm
    - liquid water content: 0.2 g/m^3
    - temperature: -4.5°C
    - impact speed: 3.6 m/s
  - 300 splinters are produced for every μg of accumulated rime

Riming

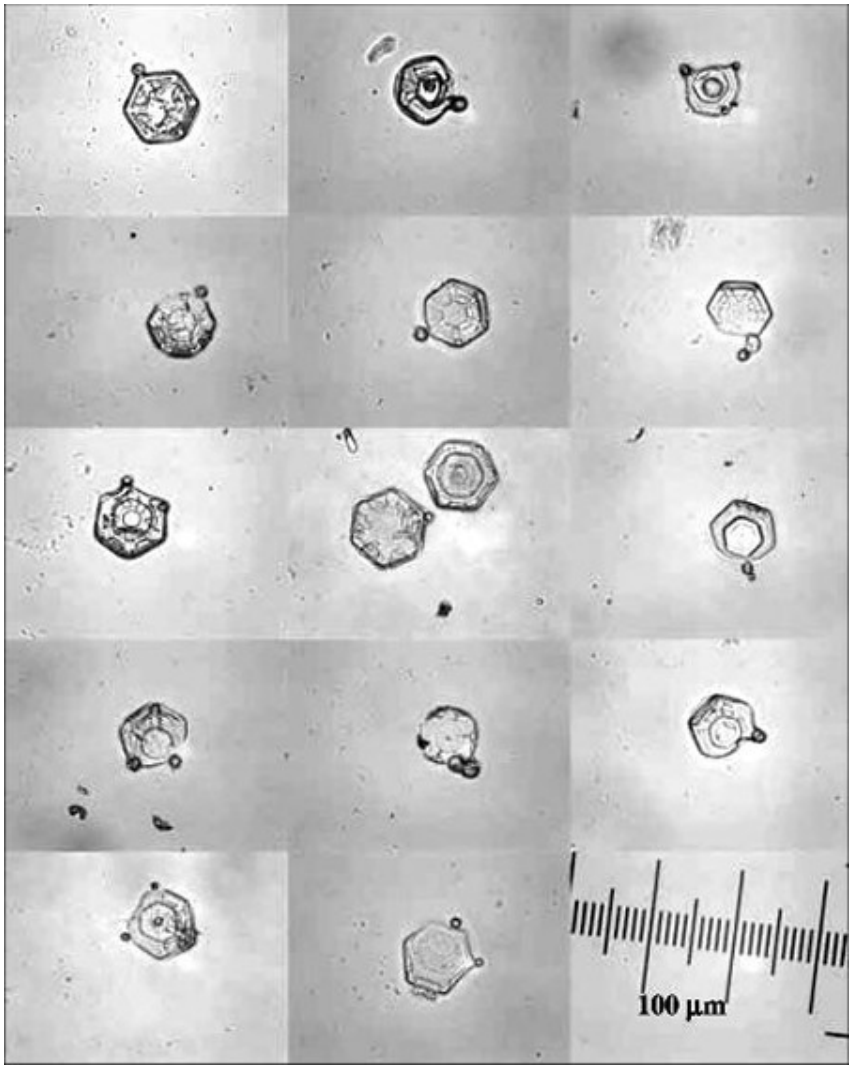

from Avila et al., 2009

Growth from the vapor phase in mixed-phase clouds

- mixed-phase cloud is dominated by super-cooled droplets
- air is close to saturated w.r.t. liquid water
- air is supersaturated w.r.t. ice

Example

T=-10°C, $RH_l \approx 100\%$, $RH_i \approx 110\%$
T=-20°C, $RH_l \approx 100\%$, $RH_i \approx 121\%$
$\Rightarrow$much greater supersaturations than in warm clouds

In mixed-phase clouds, ice particles grow from vapor phase much more rapidly than droplets.

Growth of ice crystal in supercooled water droplets

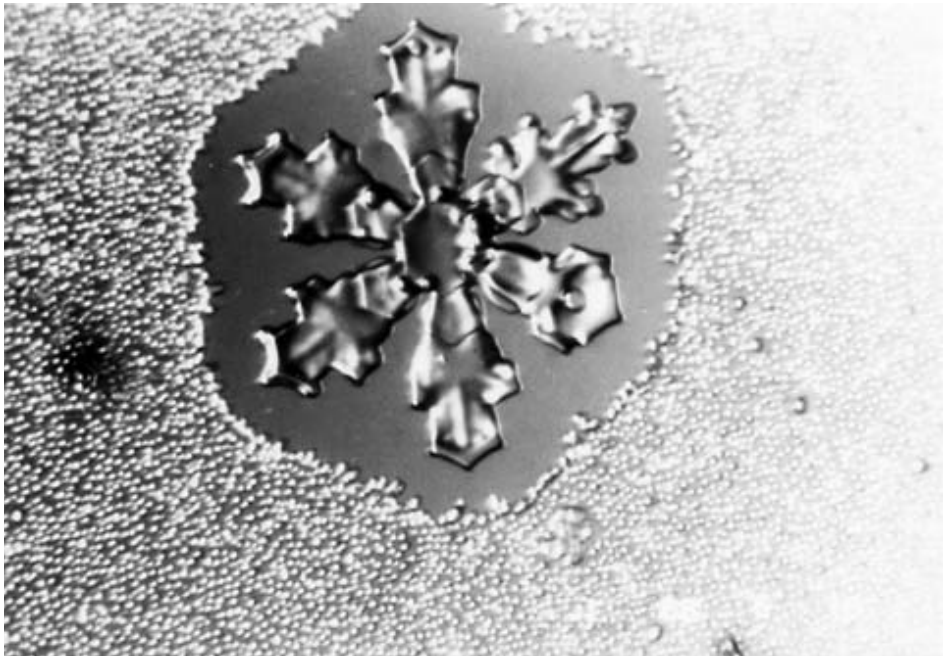

Figure from Wallace and Hobbs

growing ice crystal lowers vapor pressure in its vinvinity below saturation

$\Rightarrow$droplets evaporate

Mixed-phase cumulus clouds

Figure from Wallace and Hobbs

- cumulus turrets containing relatively large ice crystals and have fuzzy boundaries
- turrets containing small water droplets have well defined sharper boundaries

Fallstreaks of ice crystals

Figure from Wallace and Hobbs

- since equilibrium vapor pressure over ice is lower than over water, ice crystals evaporate slower and may migrate for larger distances into subsaturated air surrounding the cloud
- large ice crystals may fall out of clouds and survive great distances before they evaporate completely, even if ambient air is subsaturated w.r.t. ice
- trails of ice are called fallstreaks or virga

Shapes of ice crystals

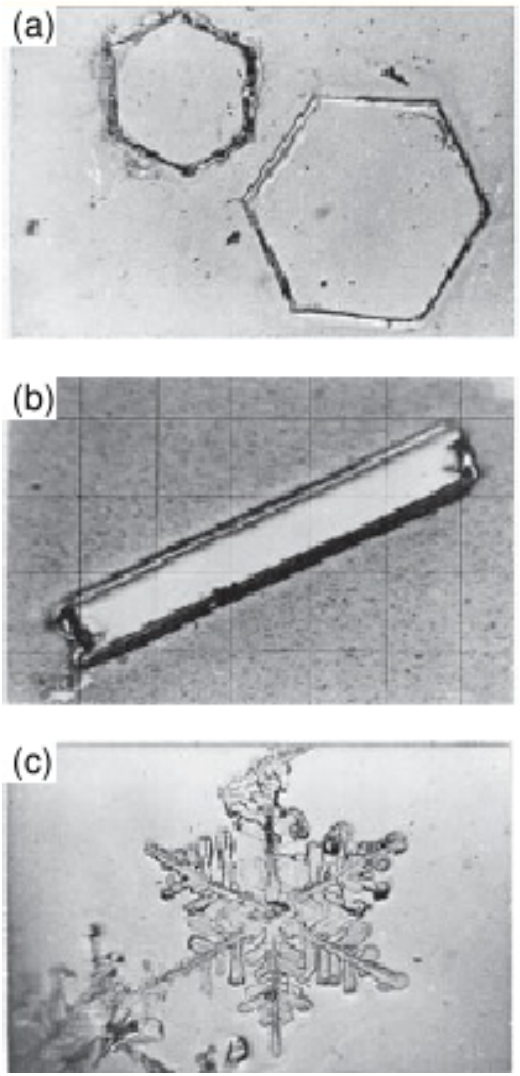

Figure from Wallace and Hobbs

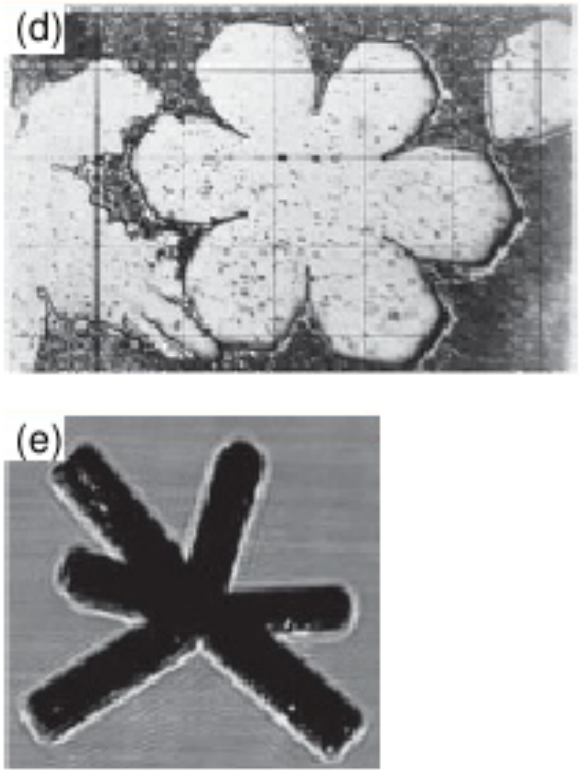

Fig. 6.40 Ice crystals grown from the vapor phase: (a) hexagonal plates, (b) column, (c) dendrite, and (d) sector plate. [Photographs courtesy of Cloud and Aerosol Research Group, University of Washington.] (e) Bullet rosette. [Photograph courtesy of A. Heymsfield.]

Mass growth rate of an ice crystal

- diffusional growth of ice crystal similar to growth of droplet by condensation
- more complicated, mainly because ice crystals are not spherical $\Rightarrow$points of equal water vapor do not lie on a sphere centered on crystal

$$\frac{dM}{dt} = 4\pi C D \left(\rho_v(\infty) - \rho_{vc}\right)$$

Mass growth rate of an ice crystal

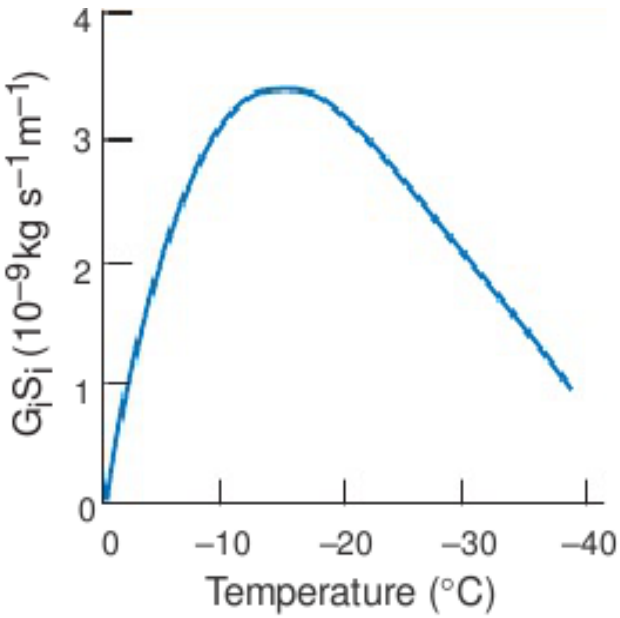

Fig. 6.39 Variation of G_iS_i [see Eq. (6.37)] with temperature for an ice crystal growing in a water-saturated environment at a total pressure of 1000 hPa.

Figure from Wallace and Hobbs

Approximate form:

$$\frac{dM}{dt} = 4\pi C G_i S_i$$

- Maximum growth rate at about -14°C

Mass growth rate of an ice crystal

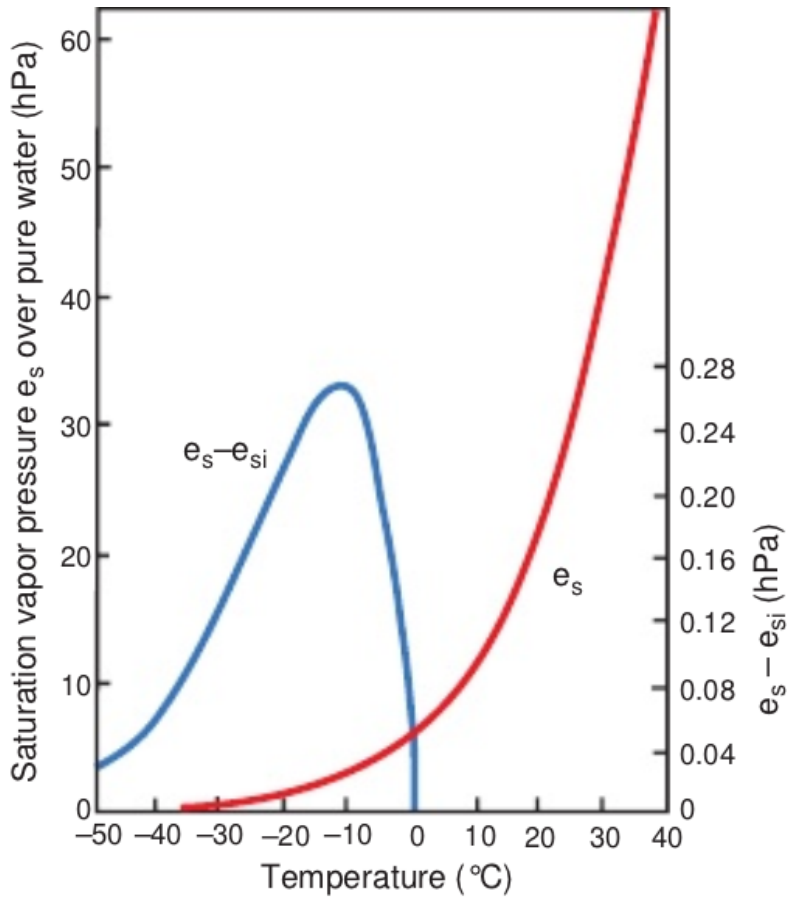

Fig. 3.9 Variations with temperature of the saturation (i.e., equilibrium) vapor pressure e_s over a plane surface of pure water (red line, scale at left) and the difference between e_s and the saturation vapor pressure over a plane surface of ice e_{si} (blue line, scale at right).

Figure from Wallace and Hobbs

Maximum growth rate at about -14°C

⇒difference between saturated pressures over water and ice is maximal at this temperature

⇒ice crystals grow most rapidly

Morphology diagram

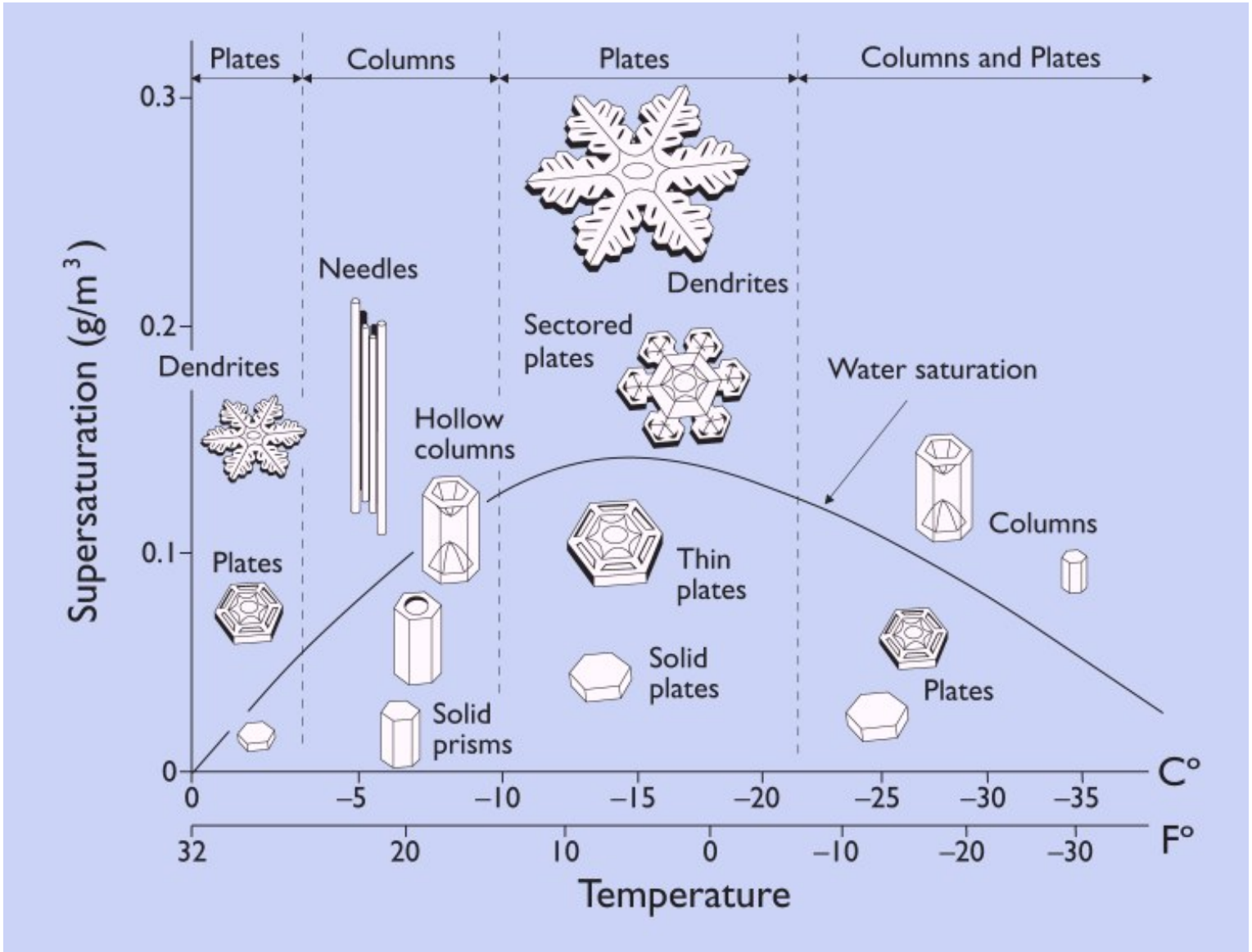

Figure from Libbrecht 2005

Growth by accretion

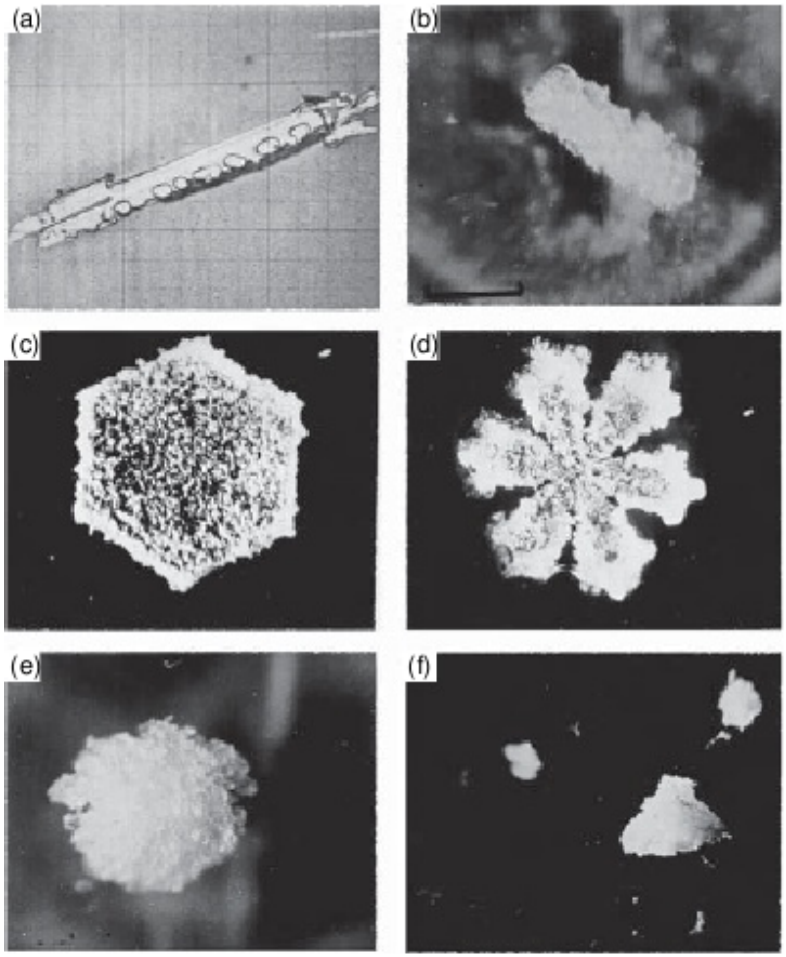

Fig. 6.41 (a) Lightly rimed needle; (b) rimed column; (c) rimed plate; (d) rimed stellar; (e) spherical graupel; and (f) conical graupel. [Photographs courtesy of Cloud and Aerosol Research Group, University of Washington.]

Figure from Wallace and Hobbs

- ice crystals falling through cloud of supercooled water droplets and other ice crystals may grow by accretion of water or of other ice crystals
- leads to rimed structures and graupel

Growth by aggregation

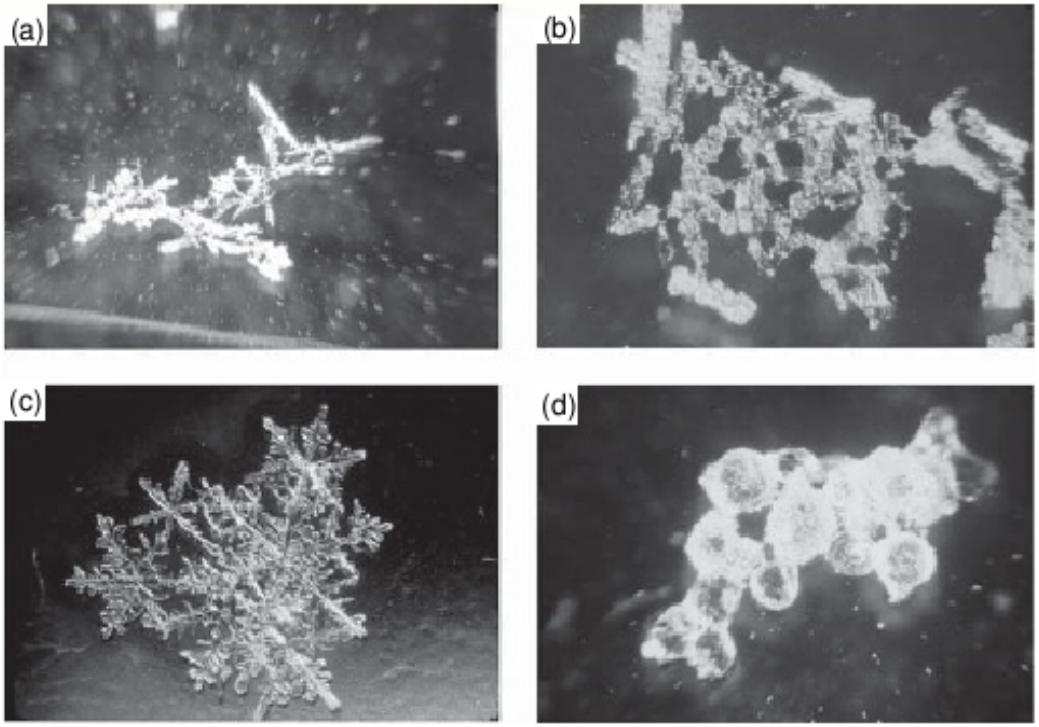

Fig. 6.44 Aggregates of (a) rimed needles; (b) rimed columns; (c) dendrites; and (d) rimed frozen drops. [Photographs courtesy of Cloud and Aerosol Research Group, University of Washington.]

Figure from Wallace and Hobbs

Snowflakes are formed by aggregation.

Collection efficiency for accretion

collection efficiency = collision efficiency $\times$ coalescence efficiency

- can be determined theoretically for simple ice plates (Pitter and Pruppacher, 1974)
  - aerodynamic calculation of trajectories of water droplets relative to ice crystals
  - coalescence efficiency ≈ 1, because ice crytals are relatively small

Collection efficiency for aggregation

- not yet determined theoretically
- observations:
  - open structures (e.g. dendrites) more likely stick to other ice crystals
  - sticking more likely at higher temperatures
- $\Rightarrow$significant aggregation only at T $>$-10°C

Mass growth rate for accretional and aggregational growth

$$\frac{dm}{dt} = \bar{E} w_l \pi R^2 (v(R) - v(r))$$

$\bar{E}$ – mean collection efficiency
w_l – cloud liquid water content
v – fall speed of crystals / droplets
R – radius of collector crystal
r – radius of supercooled droplets

Same approach for aggregation, with w_l replaced by w_i (ice water content).

Formation of precipitation in cold clouds

- 1789: Franklin suggested that “much of what is rain, when it arrives at the surface of the Earth might have been snow, when it began its descent ...”
- 1911: Wegener stated that ice particles grow preferentially by deposition from the water phase in mixed phase clouds.
- 1933: Bergeron, 1938: Findeisen
  First quantitative studies of formation of precipitation in cold clouds

Bergeron-Findeisen Process

1. Deposition from vapor phase
2. Riming / aggregation

$\Rightarrow$precipitation sized particles can be produced in reasonable time periods.

Field experiments

- several field experiments were performed in the last years: e.g. CRYSTAL-FACE, INCA, TC4 ...
- provide information about cloud microphysics at specific points in the cloud, usually no measurements of vertical structure
- can not characterize evolution of cloud microphysics spatial and temporal structure, and link these characteristics to environmental factors (available CCN)

Remote sensing methods

- Precipitation radar: vertical development of precipitation sized droplets in clouds, information on thermodynamic phase of hydrometeors
- Cloud radar (millimeter wavelength): cloud boundaries (bottom and top), small droplets not measured
- Satellite images (visible, NIR): Provide information about optical thickness and particle size (at cloud top).
  - Polar orbit (e.g. MODIS): relatively good spatial resolution (1km), but poor temporal resolution
  - Geostationary orbit (e.g. MSG): good temporal resolution (up to 5 min), but poor spatial resolution (5km)

Conceptual diagram of microphysical stages

diagram describes 5 microphysical stages (droplet growth by diffusion, collision-coalescence, warm rainout, ice-water mixed phase, glaciated phase)

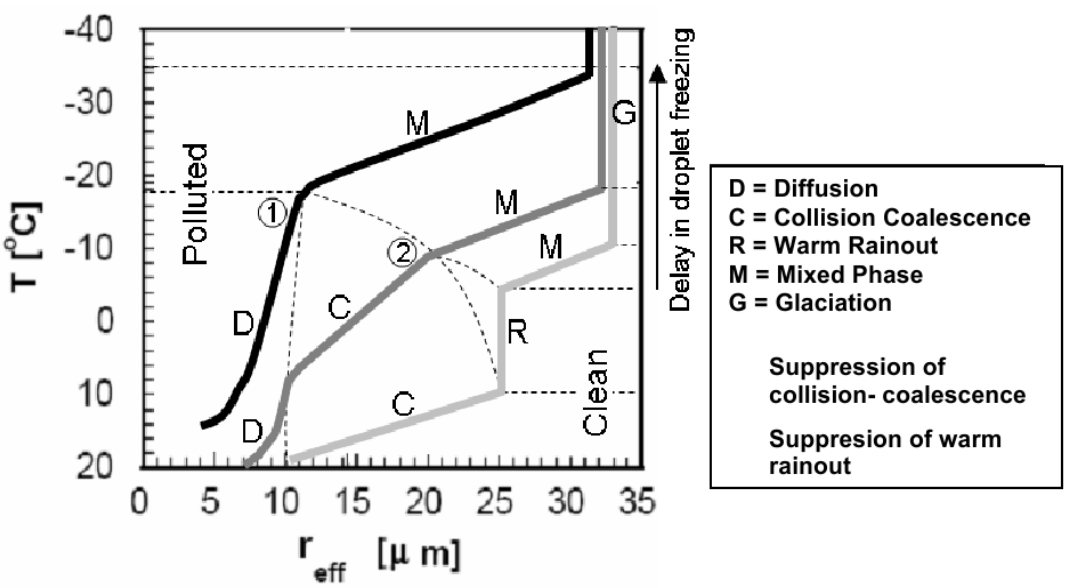

Figure from Martins et al., 2011,
adapted from Rosenfeld and Woodley, 2003

- bottom curve: maritime environment with low CCN concentration (possibility of warm rainout)
- middle curve: continental case, large number of CCN suppress warm rain, glaciation starts at slightly lower T
- top curve: polluted environment where very large number of CCNs produce numerous small droplets at cloud base, supressing collision-coalescence, freezing starts at even lower T

Cloud side remote sensing

- vertical profile of effective radius: very sensitive to aerosol environment
- brightness temperature profile: can directly be associated with thermodynamic phase, provides information on the glaciation temperature
- high temporal resolution: Evolution of cloud microphysics can be observed

First cloud side measurements

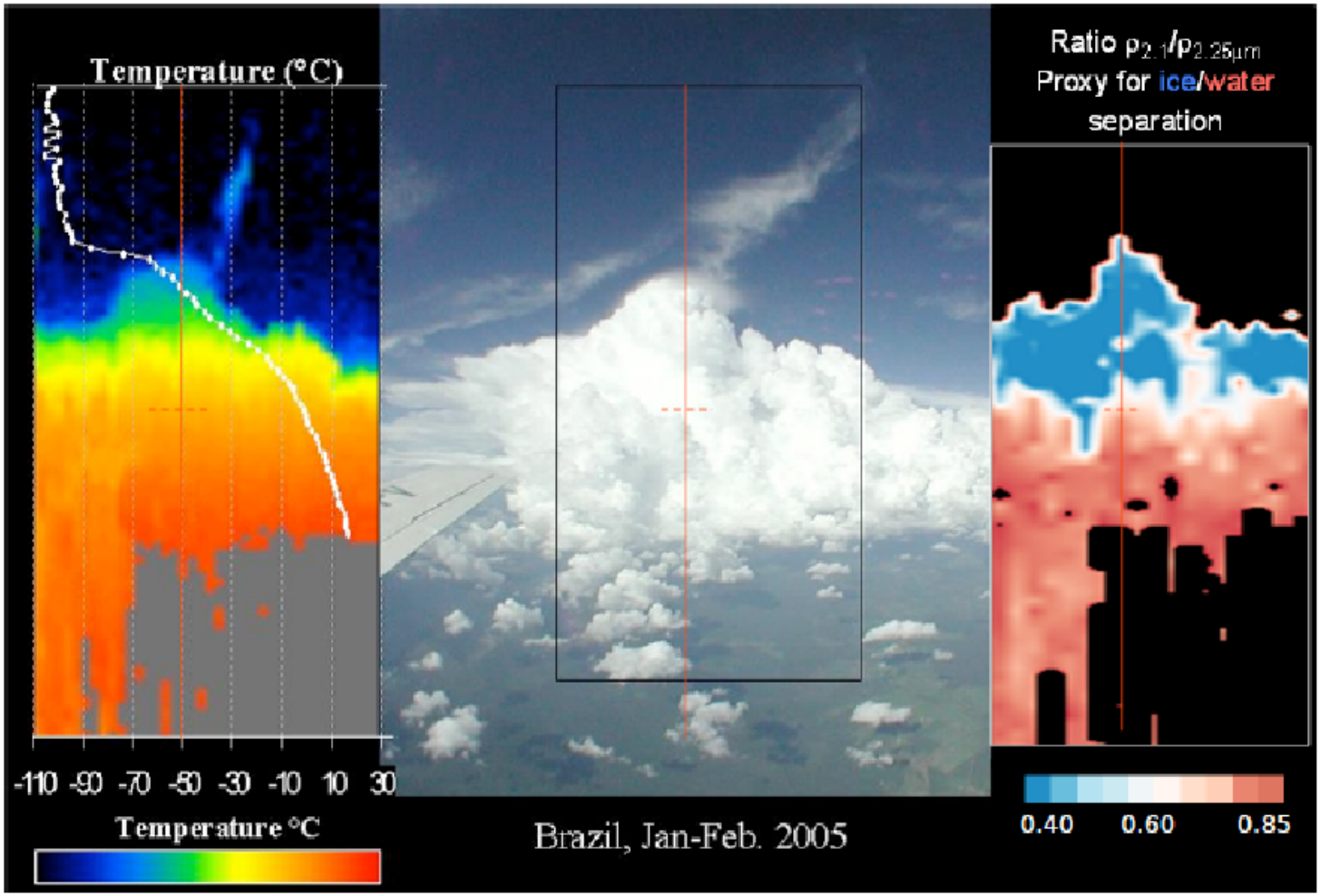

Figure from Martins et al., 2011

Retrieval of effective radius and cloud phase

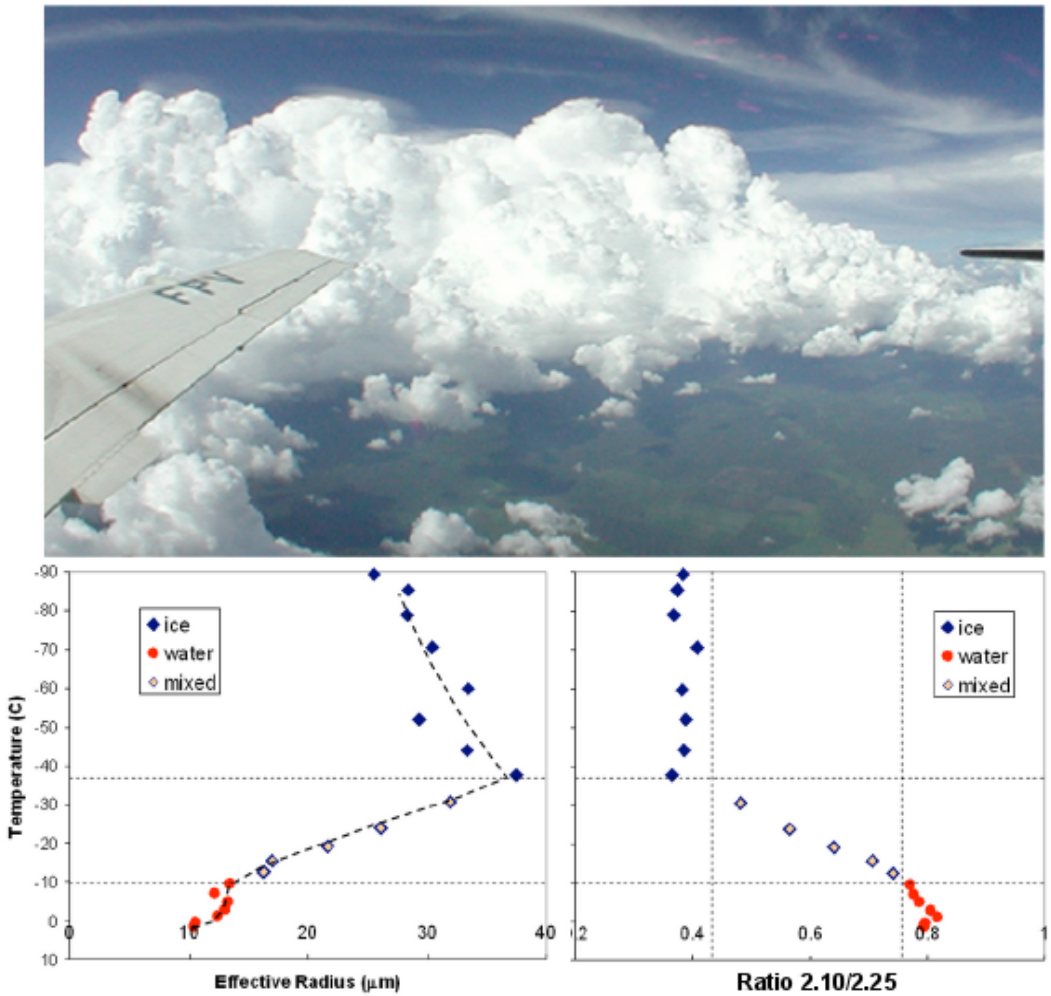

Figure from Martins et al., 2011

MYSTIC simulation of cloud scanner observation

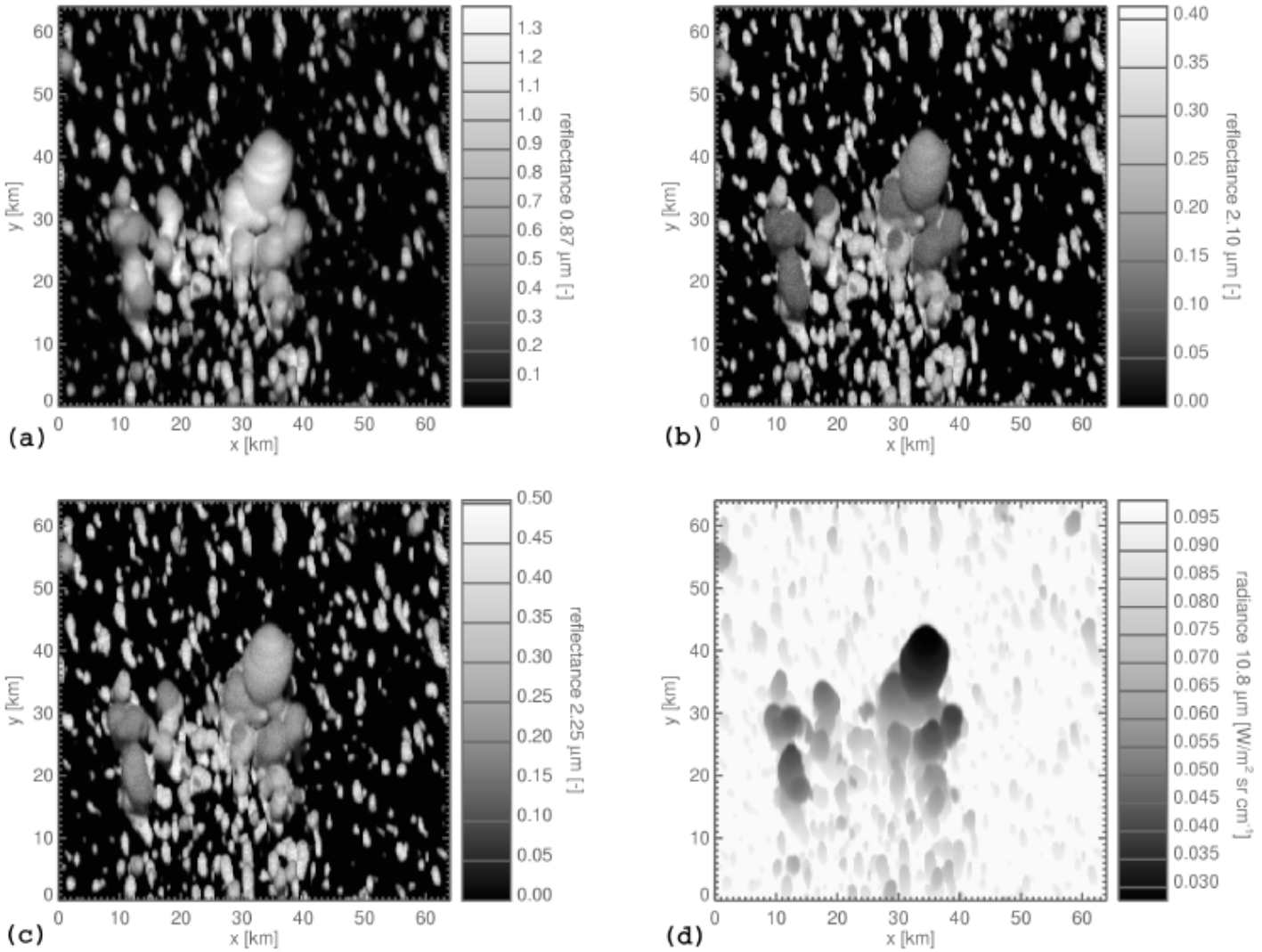

Figure from Zinner et al., 2008

Cloud observation system at MIM

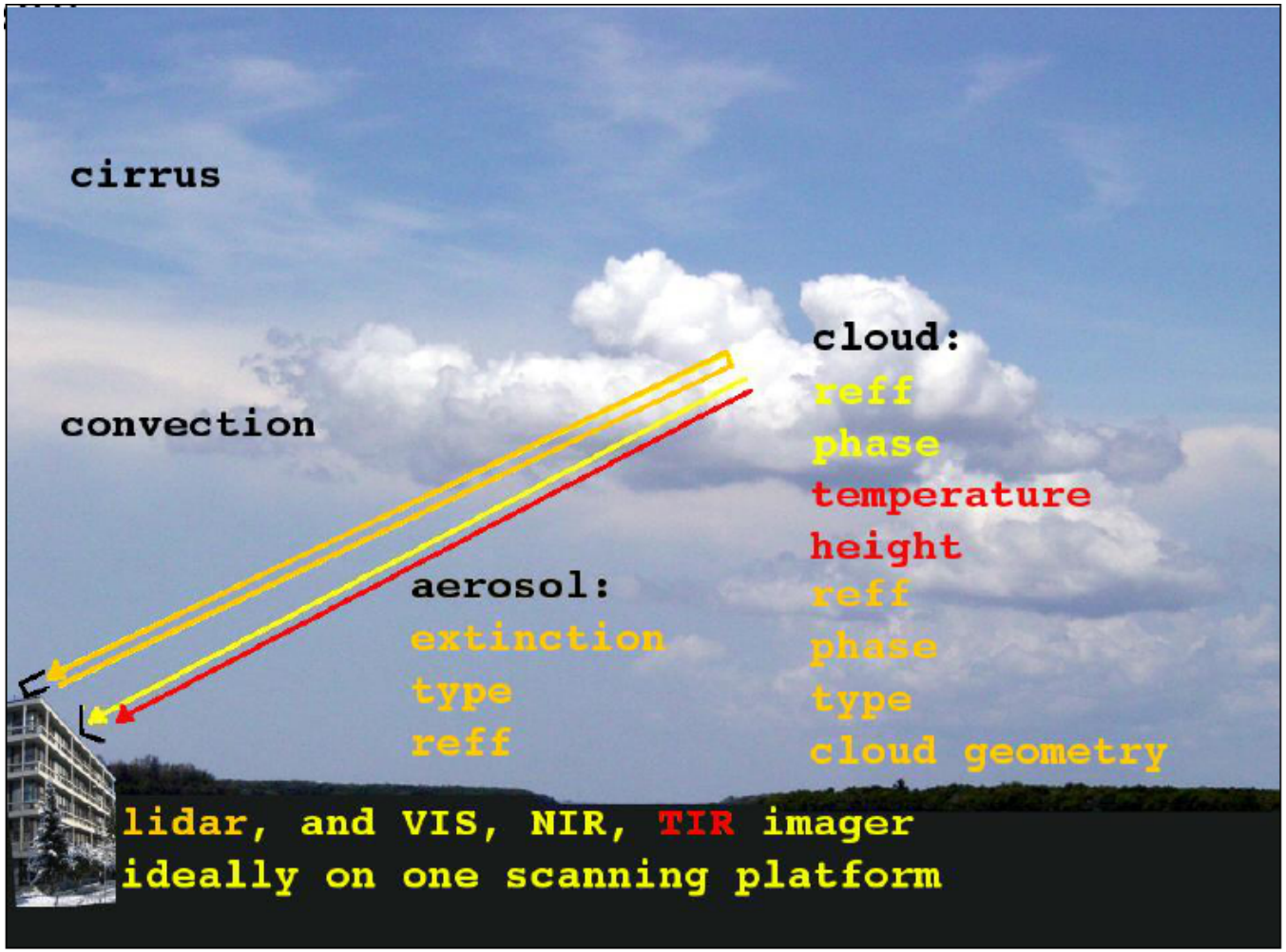

Figure from Zinner et al., Poster EGU 2009